U.S. DEPARTMENT OF COMMERCE
National Technical Information Service

PB-257 514

Environmental Aerosol Measurements Using an Airborne Particle Morphokinetometer

Spectron Development Labs, Inc, Tullahoma, Tenn

Prepared for

Environmental Sciences Research Lab, Research Triangle Park, N C Aerosol Research Branch

Aug 76

266146.

PB 257 514

EPA-600/3-76-087
August 1976

Ecological Research Series

REPRODUCED BY
NATIONAL TECHNICAL
INFORMATION SERVICE
U. S. DEPARTMENT OF COMMERCE
SPRINGFIELD, VA. 22161

TECHNICAL REPORT DATA

(Please read Instructions on the reverse before completing)

1. REPORT NO. EPA-600/4-76-087	2.
3. RECIPIENT'S ACCESSION NO.	
4. TITLE AND SUBTITLE: ENVIRONMENTAL AEROSOL MEASUREMENTS USING AN AIRBORNE PARTICLE MORPHOKINETOMETER	5. REPORT DATE: August 1976
	6. PERFORMING ORGANIZATION CODE
7. AUTHOR(S): W.M. Farmer and J.O. Hornkohl	8. PERFORMING ORGANIZATION REPORT NO.
9. PERFORMING ORGANIZATION NAME AND ADDRESS: Spectron Development Laboratories, Inc. P.O. Box 861 Tullahoma, TN 37388	10. PROGRAM ELEMENT NO. 1AA603
	11. CONTRACT/GRANT NO. DA-6-99-2294A
12. SPONSORING AGENCY NAME AND ADDRESS: Environmental Sciences Research Laboratory Office of Research and Development U.S. Environmental Protection Agency Research Triangle Park, NC 27711	13. TYPE OF REPORT AND PERIOD COVERED: Final 11/75 - 2/76
	14. SPONSORING AGENCY CODE: EPA-ORD

15. SUPPLEMENTARY NOTES

16. ABSTRACT

Measurements of ambient aerosols using an airborne particle morphokinetometer are described. The measurements were of large particles (greater than 5 micrometers in diameter) in environmental aerosols around Phoenix, Arizona, during November 1975. Speed of the sample space on the airborne platform and time resolved measurements of relative particle number density and particle size distributions for horizontal and vertical flight profiles were obtained. The results show that the large aerosol particles were predominantly 50-75 micrometers in size, that the relative number density could vary greatly in space and time, and that the largest concentration of particles were within 28 meters of ground level.

17. KEY WORDS AND DOCUMENT ANALYSIS

a. DESCRIPTORS	b. IDENTIFIERS/OPEN ENDED TERMS	c. COSATI Field/Group
*Air Pollution	Phoenix, AZ	13B
*Aerosols		07D
*Particle size distribution		14B
Velocity measurement		20F
*Interferometers		20E
*Lasers		

18. DISTRIBUTION STATEMENT: RELEASE TO PUBLIC	19. SECURITY CLASS (This Report): UNCLASSIFIED 20. SECURITY CLASS (This page): UNCLASSIFIED	21. NO. OF PAGES: 96 22. PRICE: $5.00/2.25

EPA Form 2220-1 (9-73)

PRICES SUBJECT TO CHANGE

EPA-600/3-76-087
August 1976

ENVIRONMENTAL AEROSOL MEASUREMENTS

USING AN AIRBORNE PARTICLE MORPHOKINETOMETER

by

W.M. Farmer and J.O. Hornkohl
Spectron Development Laboratories, Inc.
Tullahoma, Tennessee 37388

DA-6-99-2294A

Project Officer

Jack L. Durham
Aerosol Research Branch
Environmental Science and Research Laboratory
Research Triangle Park, NC 27711

U.S. ENVIRONMENTAL PROTECTION AGENCY
OFFICE OF RESEARCH AND DEVELOPMENT
ENVIRONMENTAL SCIENCES RESEARCH LABORATORY
RESEARCH TRIANGLE PARK, NC 27711

DISCLAIMER

This report has been reviewed by the Environmental Science and Research Laboratory, U.S. Environmental Protection Agency, and approved for publication. Approval does not signify that the contents necessarily reflect the views and policies of the U.S. Environmental Protection Agency, nor does mention of trade names or commercial products constitute endorsement or recommendation for use.

ABSTRACT

Measurements of ambient aerosols using an airborne particle morphokinetometer are described. The measurements were of large particles (greater than 5 micrometers in diameter) in environmental aerosols around Phoenix, Arizona, during November 1975. Speed of the sample space on the airborne platform and time resolved measurements of relative particle number density and particle size distributions for horizontal and vertical flight profiles were obtained. The results show that the large aerosol particles were predominantly 50-75 micrometers in size, that the relative number density could vary greatly in space and time, and that the largest concentration of particles were within 28 meters of ground level.

CONTENTS

		Page
Abstract		iii
List of Figures		vi
List of Tables		ix
I	Introduction	1
II	Summary	5
III	Conclusions	7
IV	Recommendations	9
V	PM Signal Analysis for Determination of Particle Size	11
VI	The SDL Particle Morphokinetometer	21
VII	Results	35
VIII	Calibration and Error Analysis	79
References		85
Appendix. Daily Log		87

Preceding page blank

LIST OF FIGURES

Number		Page
1	Generation of Free Space Interference Fringes with a Laser Doppler Velocimeter System	2
2	Huygen's Diagram of Interference Fringe Generation in PM Probe Volume	12
3	Visibility as a Function of D/δ for Two Particel Shapes	15
4	Uncertainty in Spherical Particle Diameters for Various Values of Uncertainty in the Visibility	17
5	¥2700 FF 500. Channel 3 Forward and Backscatter Observation Modes	22
6	¥2700 Model B. As Flown on the EPA Helicopter	23
7	Optical System Installation on the EPA Helicopter	25
8	PMAC 554 Signal Processing Electronics	26
9	Block Schematic of the Signal Processing Electronics	28
10	DC Integrator Circuit	29
11	AC Integrator Circuit	31
12	November 19. Histogram From Instrumentation Test Flight	38
13	November 19. Particle Size Distribution Obtained During Instrument Test Operation Flight	39
14	November 22. Histogram 7, Flight 1. Particle Size Distribution	43
15	November 22. Ground Test After Second Flight	44
16	November 24. Histogram 3, Flight 1. Particle Size Distribution	47
17	November 24. Histogram 4, Flight 1. Particle Size Distribution	48

LIST OF FIGURES

Number		Page
18	November 24. Histogram 2, Flight 1. Particle Size Distribution	49
19	Signal Time Period Distribution for Velocity Determination	51
20	November 24, Flight 2. Return to Airport.	52
21	November 24, 0600 hours. Inversion Layer Histogram For 27.9 - 15.2 m Altitude Increment	54
22	November 24, 0600 hours. Inversion Layer Histogram For 13.9 - 1.3 m Altitude Increment.	55
23	November 24. Ground Based Measurement Immediately After First Flight	56
24	November 25. Flight 2. Signal Time Period Distribution for Velocity Determination	58
25	November 25. Flight 1. Track 11, 152 meters AGL Altitude	60
26	November 25. Histogram 1, Flight 1.	61
27	November 25. Histogram 2, Flight 1	62
28	November 25. Histogram 3, Flight 1	63
29	November 25. Histogram 4, Flight 1	64
30	November 25. Flight 1. Last Track East of Phoenix	65
31	November 25. Histogram 8, Flight 1.	66
32	November 25. Histogram 9, Flight 1.	67
33	November 25. Histogram 7, Flight 1.	68
34	November 25. Histogram 8, Flight 1.	69
35	November 25. Histogram 9, Flight 1.	70

LIST OF FIGURES

Number		Page
36	November 25, Flight 2	73
37	November 25. Histogram 1, Flight 2	74
38	November 25. Histogram 2, Flight 2	75
39	November 25. Histogram 5, Flight 2	76
40	November 25. Histogram 6, Flight 2	77
41	November 25, Flight 2. Track 11 (Glendale)	78

LIST OF TABLES

Number		Page
1	Doppler Period Processor	32
2	Visibility Processor	33
3	Histogram Generator	34
4	Most Frequently Occurring Particle Size as a Function of Altitude for 1600 Hours, November 19, 1975	37
5	November 22, Flight 1. PM System Data Summary	40
6	November 22, Flight 2. PM System Data Summary	41
7	November 24, Flight 1. PM System Data Summary	45
8	November 24, Flight 2. PM System Data Summary	46
9	November 25, Flight 1. PM System Data Summary	59
10	November 25, Flight 2. PM System Data Summary	71

SECTION I

INTRODUCTION

A number of different techniques can be used to measure large particles (greater than about 10 micrometers in diameter) found in environmental aerosols. Considerable difficulty exists, however, in using these techniques accurately from an airborne platform. Large errors often result from the fact that a mechanical probe must be inserted into the airstream in order to sample the aerosol. These errors result from impaction and settling in the sample line for particles greater than about 5 micrometers. Therefore, the need exists for a device which can measure such particles without the constraints imposed by mechanical sampling procedures.

During the past ten years, a laser interferometer system has been developed and successfully applied to a wide variety of applications involving the measurement of particle speeds in fluid environments ranging from water flows in pipes to high speed wind tunnels. [1-5] The utility of these instruments arises from the fact that they are highly accurate, perform perturbationless measurements with exceptionally high spatial resolution and they can function in severe environments where mechanical measurements are impossible. One instrument design, as illustrated in Figure 1, has found particularly wide acceptance because of its versatility, simplicity, and insensitivity to vibration.

Light from the laser is split into two beams of equal intensity. These beams are brought to a simultaneous cross-focus region where a set of bright and dark interference fringes are generated. Particles passing through the interference fringes scatter light which is observed with a collecting lens and photodetector. The current generated in the photodetector by the scattered light is sinusoidal with a frequency directly proportional to particle speed.

Research has conclusively, both theoretically and experimentally, demonstrated that in addition to a speed measurement with such interferometer systems, it is also possible to determine the size of the particle by measurement of the relative signal shape. [6-8] Since such a measurement is obtained as a ratio of signal parameters, the size determination is independent of absolute signal magnitude. Hence, there is no need to calibrate either the laser for power output or the photodetector for amplitude response in order to determine particle size. Since particle size and speed can be simultaneously measured, particle mass concentration can be determined when particle density is known and the instrumental sample space is calibrated. Thus,

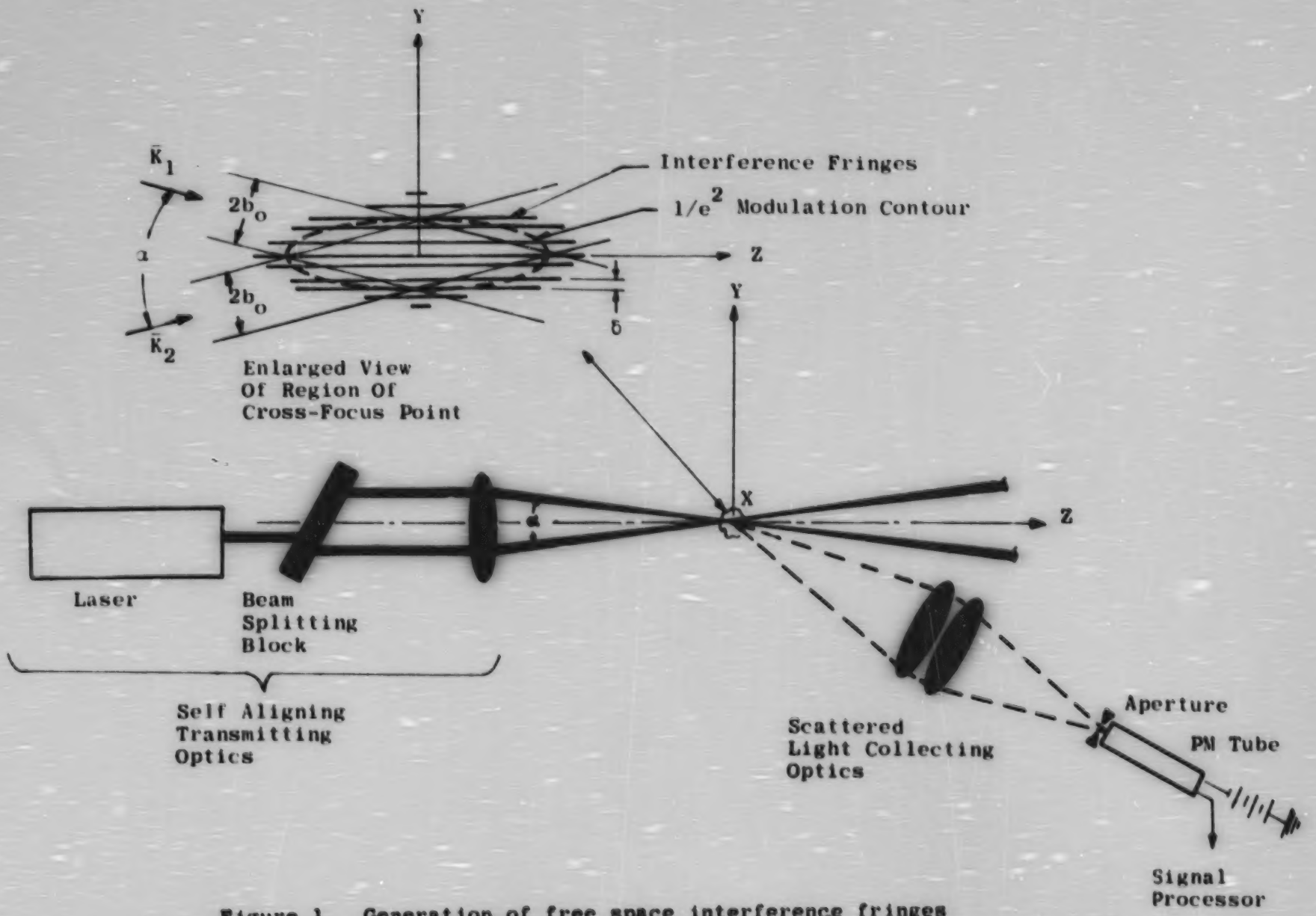

Figure 1. Generation of free space interference fringes with a laser Doppler velocimeter system.

it appears that such a system should be capable of obtaining particle size measurements where mechanical probes would be limited by losses in the sampling line.

Spectron Development Laboratory (SDL) personnel have successfully worked with such interferometer systems for a number of years in a wide variety of applications. [9-12] As a result of that experience, SDL has developed an instrument which is capable of optically measuring particle size and velocity and sorts the acquired data into histogram formats that allow convenient statistical analysis. Since the device can measure parameters relative to shape and speed of the particle, SDL has chosen to call its device a "particle morphokinetometer" (PM).

A need arose for the Environmental Protection Agency (EPA) to determine the nature of the atmospheric aerosol content in the Phoenix, Arizona area. In order to provide measurements of the large particles which might be present during the study, SDL was requested to install and maintain its instrument on the EPA helicopter used for the airborne aerosol measurements. This application is believed to be the first time that such an instrument has been used successfully to obtain these kinds of measurements from an airborne platform.

This report summarizes the results of the measurements so obtained with the SDL instrument.

Section V provides a discussion of the principles utilized in the SDL instrumentation. A detailed description of the operating characteristics of the device and its installation on the helicopter is given in Section VI. A summary and discussion of the data obtained is presented in Section VII. Section VIII discusses possible instrument calibration tests and error sources in the measurements. Appendix A provides a daily operations log kept by SDL personnel in order to give the reader some insight into how the instrument was operated and tested and the problems encountered in this initial application.

SECTION II

SUMMARY

The SDL particle morphokinetometer has been successfully operated from an airborne platform in Phoenix, Arizona. Data were obtained on six different flights and under a variety of environmental conditions including day and nighttime operation. Both velocity and particle size distributions were obtained at two different positions relative to the aircraft. Time resolved particle size and relative number density measurements were obtained for horizontal and vertical sample directions. The horizontal sample revealed number density variations as large as factors of 2 or 3 for sample path differentials as small as 0.4 Km and factors as large as 100 for the overall sample. The vertical sample, taken during the early morning hours of November 24, revealed a very shallow inversion layer between 15 and 30 m. The relative number density in the inversion layer was about 100 times that measured above it. Measured mean particle sizes ranged between 50 and greater than 75 μm in diameter. The velocity measurements yielded a value of 12.5 ± 4.9 m/sec. at a distance of approximately 66 cm from the edge of the aircraft and 9.5 ± 4 m/sec. at a distance of 40 cm.

A primary limitation of the system was found to be signal noise resulting from background sunlight. Due to the fact that an interference filter was used with too broad a passband, background sunlight caused occasional high levels of photomultiplier tube shot noise. Operation with a filter combination having a narrower bandwidth considerably improved the signal-to-noise ratio for bright sun operating conditions.

Some of the particle size data obtained by the instrument is questionable because of the smallness of the standard deviation of the size distributions and lack of the slopes in the wings of the distribution. Also the observed particle sizes on the ground covered a broader spectrum than those observed airborne. Such effects suggest that either (1) the instrument artificially biased the distributions in manners which could not be detected during calibration or ground applications, or (2) large fugitive dust sources such as farms or unpaved roads produce large particles with narrow distributions, but near paved roads (in the area of the airport), tire action crushes the mineral, yielding smaller particles with a greater dispersion.

Preceding page blank

SECTION III

CONCLUSIONS

It has been clearly demonstrated that a PM system can function from the EPA helicopter without any major technical difficulties. Shock mounting for the optical system proved to be adequate, and all power inputs were sufficient.

The instrument should be positioned on the aircraft to provide a sample space outside any flow field perturbations. In any further applications, a background light filter with a passband of 1 nanometer should be used.

The time-resolved histogram data clearly shows the high variability of atmospheric number density for horizontal and vertical sample paths. It demonstrates the need to exercise caution in estimating mass concentration from measurements taken over long time intervals; and that when long sample time measurement techniques are used, numerous repetitive samples should be obtained. The particle size distribution observed in the early morning inversion layer was nearly the same as that observed on the ground. It is, therefore, to be concluded that in that case, the particles in the first 30 m of altitude were uniformly distributed.

The overall thrust of the data also suggests the high variability of the day-to-day atmospheric particle content and the need to sample often to obtain a clear picture of such.

Preceding page blank

SECTION IV

RECOMMENDATIONS

The results of the PM system application in Phoenix suggest several recommendations if the application of these measurement devices is pursued. Specifically, it is recommended that:

(1) A second similar instrument application be attempted with a forward scatter optical system. Such a system would not be nearly as sensitive to background light (since the receiver could never point directly toward the sun) and would generate signals with much higher amplitudes. Such a system could use a smaller laser and be more compact than the one used in Phoenix.

(2) The system should be placed such that it is not exposed to external flow field interferences (boundary layer effects, struts, etc.) in order to prevent any biases which the flow field might introduce.

(3) All electronic systems should be rack mountable. The systems in the Phoenix application were rack mounted but were not originally designed to be so.

(4) If possible such tests should extend for a sufficient period of time to allow thorough data analysis between flights, and to repeat the measurements under similar atmospheric conditions in order to give a high confidence value to the creditability of the data.

(5) Studies should be pursued to determine a visibility function for randomly shaped and randomly oriented particles.

(6) In a future application, comparative measurements should be obtained between the size determination using the mean scattered intensity and the visibility measurement to provide two independent determinations of particle size.

(7) In any future application, some means should be obtained of automatically recording flight notes and data acquisition times. A tape recorder would be profitable for such requirements.

Preceding page blank

SECTION V

PM SIGNAL ANALYSIS FOR DETERMINATION OF PARTICLE SIZE

For completeness, a brief review is given of the basic principles which must be utilized to determine particle size and velocity from a measurement of signal shape and frequency.

THEORETICAL CONSIDERATIONS

Consider Figure 2. Two equal intensity, well-collimated coherent light beams intersect at a common origin (geometric center) with an included angle, α . A Huygen's diagram of the wavefronts show that planar interference fringes are generated which are perpendicular to the plane defined by the beam centerlines and are parallel to the bisector between the beams. The distance between the periodic fringes, δ , is given by:

$$\delta = \lambda/[2\sin(\alpha/2)] \tag{1}$$

where λ is the wavelength of the coherent light. The region of interference forms an ellipsoid of revolution which is a contour of constant intensity about the bisector between the beams. Particles which pass through the ellipsoid generate periodic signals. The number of cycles in the signal depends on the number of interference fringes which the particle trajectory intercepts. A maximum number of cycles is generated when the trajectory is in the plane of the beam centerlines and passes through the geometric center of the ellipsoid. Particles passing through the edge of the ellipsoid will always generate fewer cycles of information. When a particle (assumed spherical) much less than δ in diameter crosses the fringe pattern, it can be assumed to be uniformly illuminated at all points along its path through the fringe pattern, and the light which is scattered by the particle is proportional to the observable flux illuminating it. Thus, measurement of the time period, τ , of the scattered light is related to the velocity, v, of the particle through the relationship

$$v = \delta/\tau \tag{2}$$

Preceding page blank

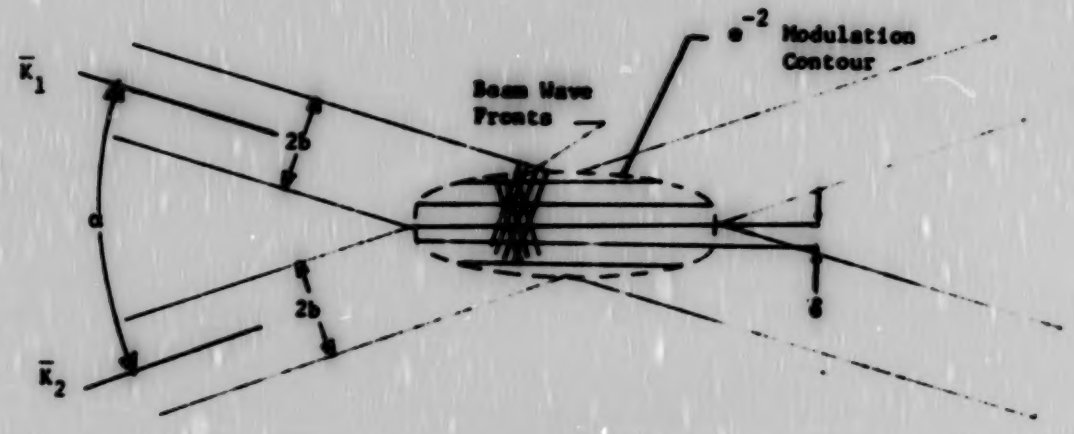

Figure 2. Huygen's Diagram Of Interference Fringe Generation In PM Probe Volume.

As the size of the scattering particle increases relative to δ, the illumination of the particle is no longer uniform and must be averaged over the cross-sectional area of the particle. The non-uniform illumination of the particle results in a reduction in the contrast or visibility of the scattered light signal. Let I_{max} be the maximum value in intensity in a period of the scattered light from a particle and I_{min} the next successive minimum. The visibility, V, can then be defined as:

$$V = \frac{I_{max} - I_{min}}{I_{max} + I_{min}} \tag{3}$$

It is straightforward to show that V is fully equivalent to the ratio of AC amplitude divided by the DC amplitude of the scattered light signal. Henceforth the high frequency "Doppler" portion of the signal will be referred to as the "AC", it usually has many cycles of information relative to that of the DC component (the DC component refers to the mean value of the Gaussian shaped low frequency term describing the signal). Analytically the visibility may be written as:

$$V \simeq \frac{\int_{A_p} I_o \cos(2\pi y/\delta) dA_p}{\int_{A_p} I_o \, dA_p} \tag{4}$$

where A_p is the cross-sectional area of the particle, I_o is intensity distribution across one of the illuminating beams, and y is the coordinate normal to the fringe planes. When I_o is a Gaussian function (TEM ooq laser beam) it can be shown that Equation 4 is an accurate approximation over a depth of field, ℓ, given by:

$$\ell \simeq 0.8 \, b/\alpha \tag{5}$$

where b is the radius of the e^{-2} intensity point in the illumination beam. For depths of field greater than ℓ, the signal visibility is a function of particle size and position in the illumination. In order to simplify Equation 4 for Gaussian beams and still maintain accuracy, it is required that the particle diameter, D, satisfy the relationship:

$$D \leq 0.2\ b \tag{6}$$

and for δ to satisfy:

$$\delta \leq 0.2\ b \tag{7}$$

Under these conditions V for a sphere can be written as:

$$V \simeq 2J_1(\pi D/\delta)/(\pi D/\delta) \tag{8}$$

where J_1 is a first order Bessel function of the first kind. For a cylinder V can be written as

$$V \simeq \sin(\pi L/\delta)/(\pi L/\delta) \tag{9}$$

Equations 8 and 9 are plotted in Figure 3 to illustrate the salient features of the visibility in particle size measurement.

Determination of particle size using a visibility measurement has a number of advantages over other optical techniques. Among the more important of these are:

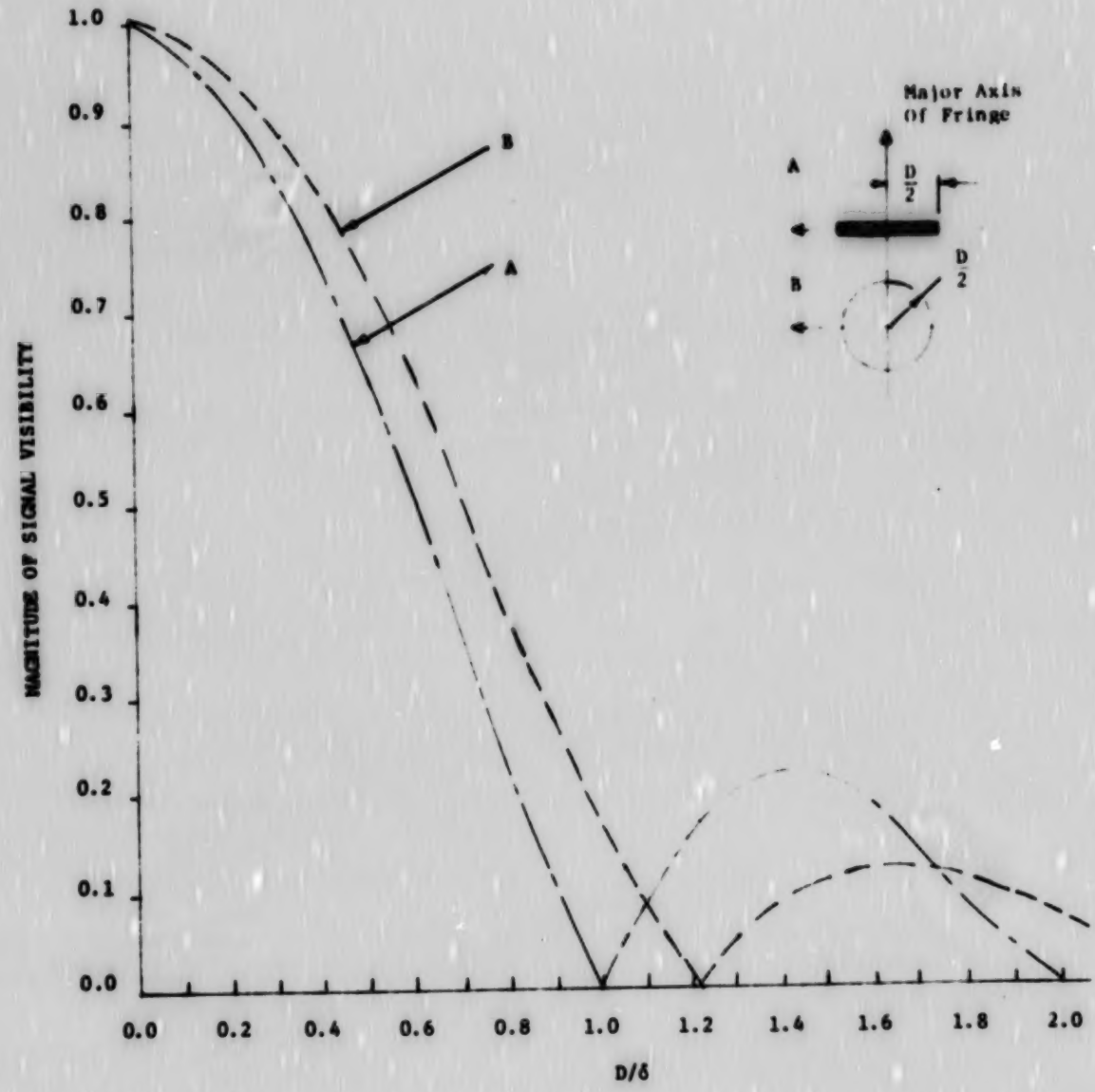

Figure 3. Visibility As A Function Of D/δ For Two Particle Shapes.

(1) High quality scattered light collecting systems are not required.

(2) A visibility measurement can determine particle size to at least ten times better than the resolution limit of the transmitting lens.

(3) With calibration, true particle flux (i.e., mass concentration) may be determined with a PM system.

(4) Size measurements may be made from backscattered light.

On the other hand, disadvantages in using this technique are also apparent. For example, design and application of a PM system must account for the facts that:

(1) Size measurement is shape dependent.

(2) High quality transmitting optical systems are required.

(3) Particle size measurement of spheres is limited to approximately a 15:1 size variation range for a given fringe period.

(4) High quality spatially coherent light is required for good interference fringe quality.

(5) The particle size measuring ability is limited by the frequency response of the signal processing electronics.

Item 5 above results from the fact that the signal frequency is velocity dependent. Hence, an instrument which measures signal visibility is limited to the measurement of particles with velocities which are less than those which produce a signal frequency greater than the frequency response limit of the instrument.

SIGNAL PROCESSING CONSIDERATIONS

To minimize error in the estimate of particle size, it is of utmost importance that signal visibility be measured with high accuracy and precision. This is due to the fact that signal visibility error and particle size error are not linearly related. For spherical particles, Figure 4 illustrates the particle diameter uncertainty for several

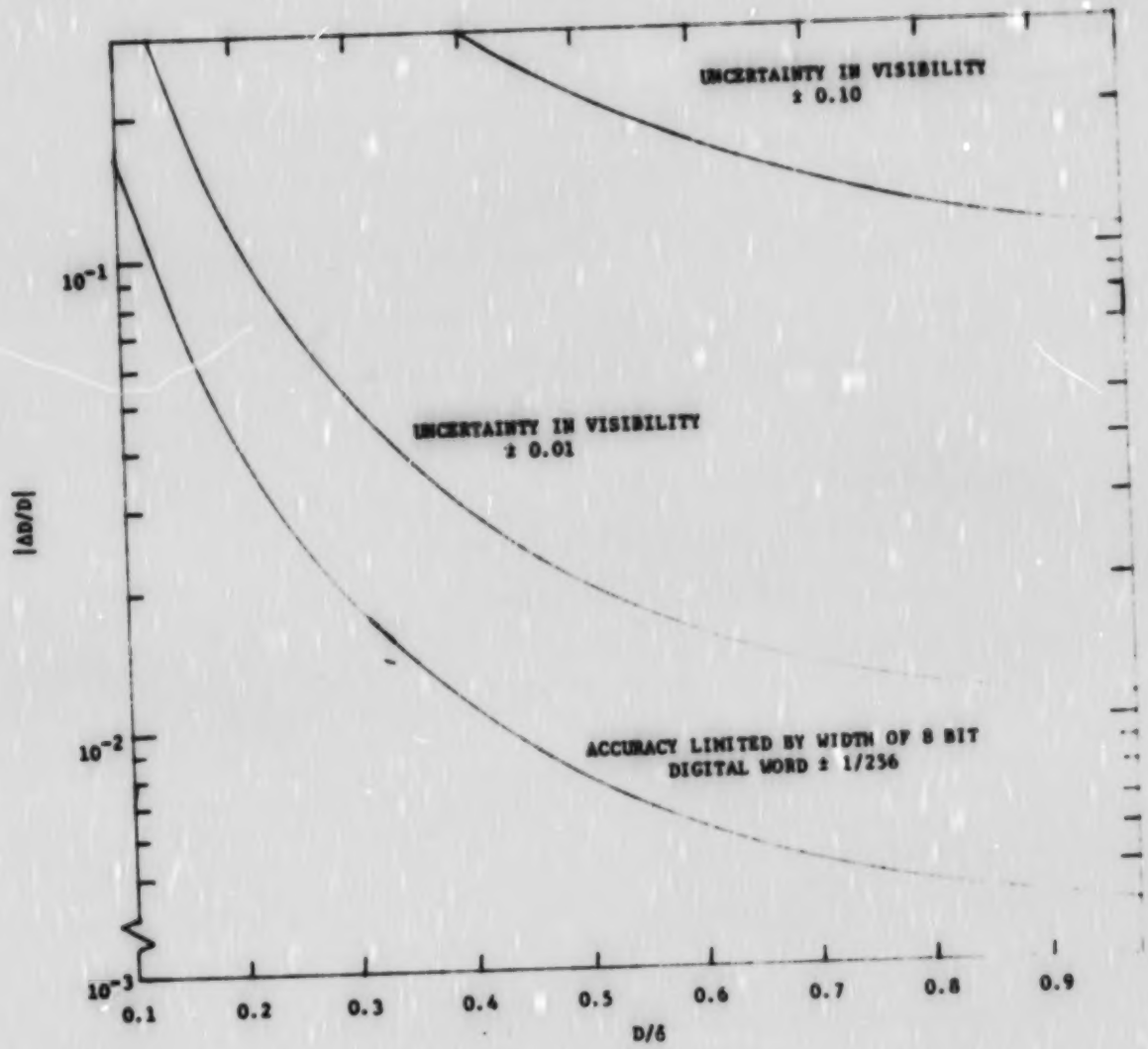

Figure 4. Uncertainty in spherical particle diameters for various values of uncertainty in the visibility.

different values of visibility. As the figure shows, where the ratio of particle diameter D to fringe period δ is near 1, the particle diameter uncertainty is the same as the visibility uncertainty. However, D/δ decreases, particle diameter uncertainty rapidly increases. Thus, when D/δ is small, the error in particle size will be much greater than that in the visibility. An instrument which measures signal visibility must seek to minimize errors in the visibility measurements if an accurate particle size measurement is to be obtained.

POTENTIAL SOURCES OF ERROR IN A SIGNAL VISIBILITY MEASUREMENT

In examining a PM signal, a number of potential error sources are evident which could produce considerable error in a visibility measurement. Among the most important error sources are:

(1) Signal noise

(2) Asymmetric signal shapes

(3) Variations in visibility in the signal

(4) Signals resulting from more than one particle

Signal noise may result from any number of sources but is usually either (1) broad band Gaussian distributed noise occurring during the entire duration of the signal, (2) single very-high-frequency spikes which occur randomly in the signal, or (3) periodic amplitude variations which mix with the signal. The first two forms of noise are usually evident when signal magnitudes are low. The third form usually results from radiative pickup from high power consuming or generating instruments operating across the entire frequency spectrum. Asymmetric signal shapes results from particles with trajectories that do not pass through the optical axis of the probe volume. Such signals can also arise through turbulence-induced distortions in the signal. Variations in signal visibility occur when D/δ is near 1, and the AC component of the signal has only a few cycles of information relative to that of the DC component. Signals resulting from more than one particle usually generate aperiodic signals of skewed shapes. Most PM optical designs account for the possibility of multiple particle signals by generating a probe volume which is small enough to produce a low probability of observing more than one particle. Certain types of error logic may also be used in the signal processing electronics to reject such signals.

VISIBILITY FROM SIGNAL INTEGRATION

In order to minimize the errors which may result from "real world" kinds of PM signals, it is most desirable to observe and measure as much of the PM signal as possible. One method of satisfying this requirement is through integration of the entire signal (within preset limits). Consider a particle whose trajectory passes through or near the geometric center of the probe volume. It can be shown that the visibility obtained by (1) computing the integral of the DC component, (2) computing the integral of the full wave rectified value of the AC component, and (3) dividing the integrated DC into the integrated AC, is (to within a known numerical factor) identical to that measured for a single cycle measured at the center of the signal. Integration of the signal is most desirable because the noise components previously listed will contribute very little to an integral value of the signal. For example, Gaussian-distributed white noise and periodic noise have zero or nearly zero values for an integration, and high frequency noise spikes contribute very little to the overall integral value. Furthermore, integration of asymmetric signals tends to reduce the effects of the asymmetry of producing an overall signal average. The primary difficulty in using a signal integration to determine the signal visibility resides in the fact that the dynamic response of an integrator will be affected by large frequency variations in the signal input. Thus, without design precautions, an integrator could produce considerable error in attempting to measure particle size in turbulent flows where there are considerable velocity variations.

SIGNAL AMPLITUDE CONSTRAINTS

While a visibility measurement is independent of signal magnitude, detailed consideration must be given to relative signal amplitude in order that a visibility measuring instrument have a sufficient dynamic range in amplitude response.

For particles of identical index of refraction and of a size greater than about 5 μm (i.e., for particles with scattering gain coefficients independent of particle size), the signal amplitude can be expected to vary by a factor of 100 over the measurable size range. Probe volume intensity variations can be expected to range over factors of 10 in each of two orthogonal probe volume dimensions. Thus, an instrument must be capable of responding to relative signal amplitude variations

of at least 10^3:1 and, more reasonably, 10^4:1. Linear amplifiers can cover a linear dynamic range of approximately 10^2 for a single range setting. The designer is thus faced with the difficulty of producing an instrument, which at one range setting can cover sufficient dynamic range to eliminate instrumental bias in particle size measurements.

One technique to overcome the dynamic range limitations is the use of logarithmic amplifiers. For example, if an integration technique is used to determine the signal visibility from a logarithmically amplified signal, it can be shown that the visibility is given by:

$$V = \text{sech}\left[\int \ln(i_{AC}) - \int \ln(i_{DC})\right] \tag{10}$$

where $\int \ln(i_{AC})$ is the integrated logarithmically amplified AC component of the signal and $\int \ln(i_{DC})$ is the integrated DC component. Logarithmic amplifiers can easily cover a dynamic range of 10^4:1 for low frequency signals, making an instrument much more sensitive to small particle signals. The primary difficulty with such amplifiers is that their sensitivity is a strong function of signal frequency and quickly decreases as the frequency increases making their effectiveness questionable for most airborne applications.

Another solution to this limitation is obtained in using the integration approach to visibility measurement. An integrator can be design to cover a 10:1 dynamic range with three digit accuracy, and 100:1 with two digit accuracy. The signal visibility processor designed by SDL personnel utilizes 4 parallel integration circuits each overlapping the other in range such that for a given signal frequency a dynamic amplitude range of 10^4:1 with three digit accuracy can be covered. Such accuracy gives an acceptable error in particle size determined by a visibility measurement even when the D/δ particle size is small.

SECTION VI

THE SDL PARTICLE MORPHOKINETOMETER

The components of the particle morphokinetometers divide naturally into two distinct subsystems - the optical system and the signal processing system. The following sections describe these subsystems and their mounting to the EPA helicopter.

THE SDL OPTICAL SYSTEM

The optical system used in this research was a slightly modified version of an optical system built by SDL called the ¥2700. The ¥2700 is built in two models, A and B. The A model uses a 5mw HeNe laser while the B model uses a 15mw laser and carries the laser and photomultiplier tube power supplies inside the optical package. The ¥2700 is designed to cover a 2700:1 particle size range using four possible channels of operation using different lens combinations. The instrument is designed to cover the size range 0.18 - 500 micrometers and can be used in a forward or backward scatter observation mode. For the helicopter application, backscatter measurements with the probe volume approximately 50 cm from the edge of the optics cabinet were to be attempted. Hence, it was decided that the ¥2700B in a channel 2 operating mode was to be used. This would provide maximum signal amplitude and, therefore, optimize the signal-to-noise ratio for the electronics system. The channel 2 lens set was arranged to provide a probe volume approximately 51 cm from the edge of the optical cabinet. In this configuration, the fringe period was 75 micrometers and a particle size range of 5 - 75 micrometers could be measured. Figure 5 schematically shows the optical system light path while Figure 6 shows a photograph of the actual instrument. The backscatter collection system utilized an F/11 lens arrangement. A slit aperture was used on the photomultiplier tube to reduce background light and eliminate possible multiple particle signals.

A 10 nanometer interference filter was originally used for background light rejection. This filter was found to be insufficient for operation on particularly bright sunny days. However, when a second 10 nanometer filter was used with the first, sufficient background light rejection appeared to be obtained.

A massive rack mount (400 kg) which was shock mounted and sat near the helicopter door provided the primary support structure for the optical system. The EPA was to furnish a small angle bracket which would allow

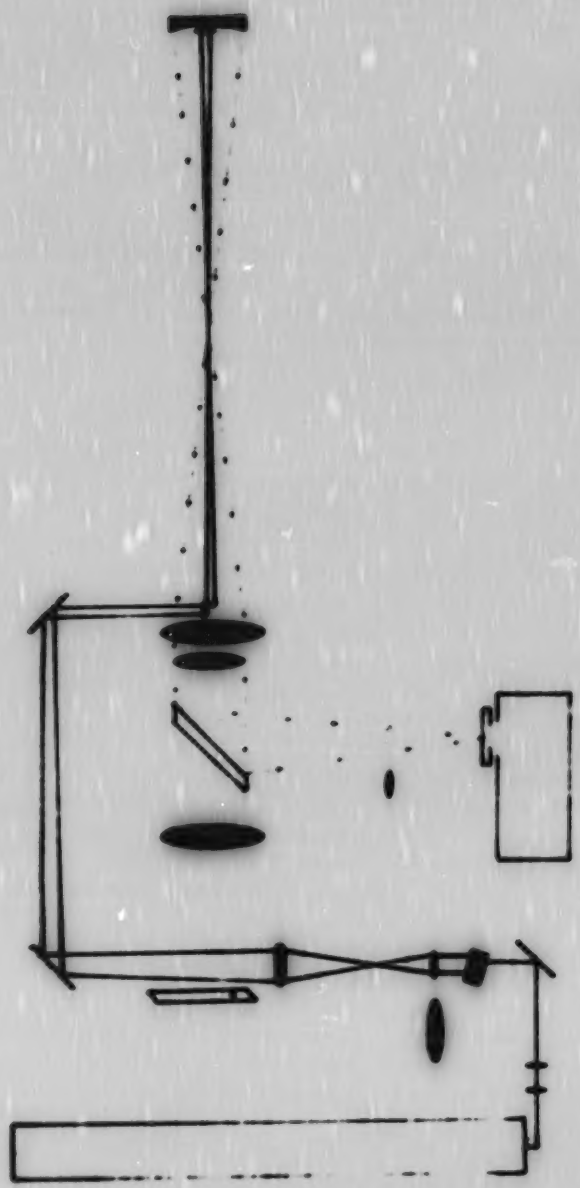

Figure 9. 2700 FF 500, Channel 3. Forward and Backscatter Observation Modes.

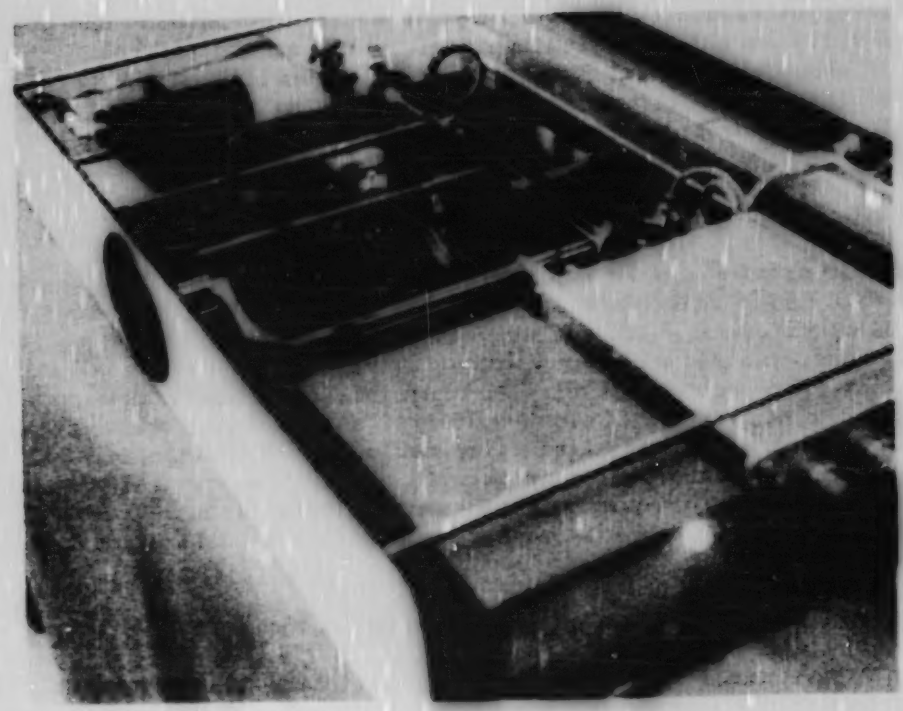

Figure 6. T2700 Model B. As Flown On The EPA Helicopter

mounting the optical system to the rack mount such that the optics cabinet protruded 10 - 12 cm outside the helicopter doorway. Preliminary tests of the optical system on the EPA bracket showed that it was not strong enough for safe flight applications. Using the EPA bracket as a pattern, SDL personnel were able to fashion one from 0.31 cm x 2.5 cm x 2.5 cm aluminum angle which was sufficient. Figure 7 shows the optical system as it was installed on the helicopter. This mounting system proved to be adequate during all flights. No optical misalignment due to helicopter vibration was ever observed.

THE SIGNAL PROCESSING ELECTRONICS SYSTEM

The SDL electronics system employed during this research is designated as the PMAC 554. This electronics system is shown in Figure 8. It contains electronics which measures the mean amplitude of the scattered light signal, the signal time period (for velocity), and the signal visibility (for particle size). In addition to the above measurements, the electronics system was also capable of sorting the acquired data into histograms of either signal time period or visibility. The histogram generator is capable of being programmed for 15 bins of arbitrary width. There are four possible normalization modes for a particle count of 10, 10^2, 10^3, or 10^4 particle measurements. The normalization modes are:

(1) A prescribed number of measurements in the total histogram.

(2) A prescribed number of measurements in the most populated bin in the histogram.

(3) A prescribed number of measurement attempts (events) regardless of the number of measurements in the histogram.

(4) A prescribed measurement time interval (0.1 - 99.9 seconds).

The instrument is designed such that an operator can terminate any histogram sequence at will or can make the instrument automatically acquire a series of histograms until commanded to stop.

The histograms acquired during the flight were recorded by a digital recorder. Two different recorders were used during the flights, a

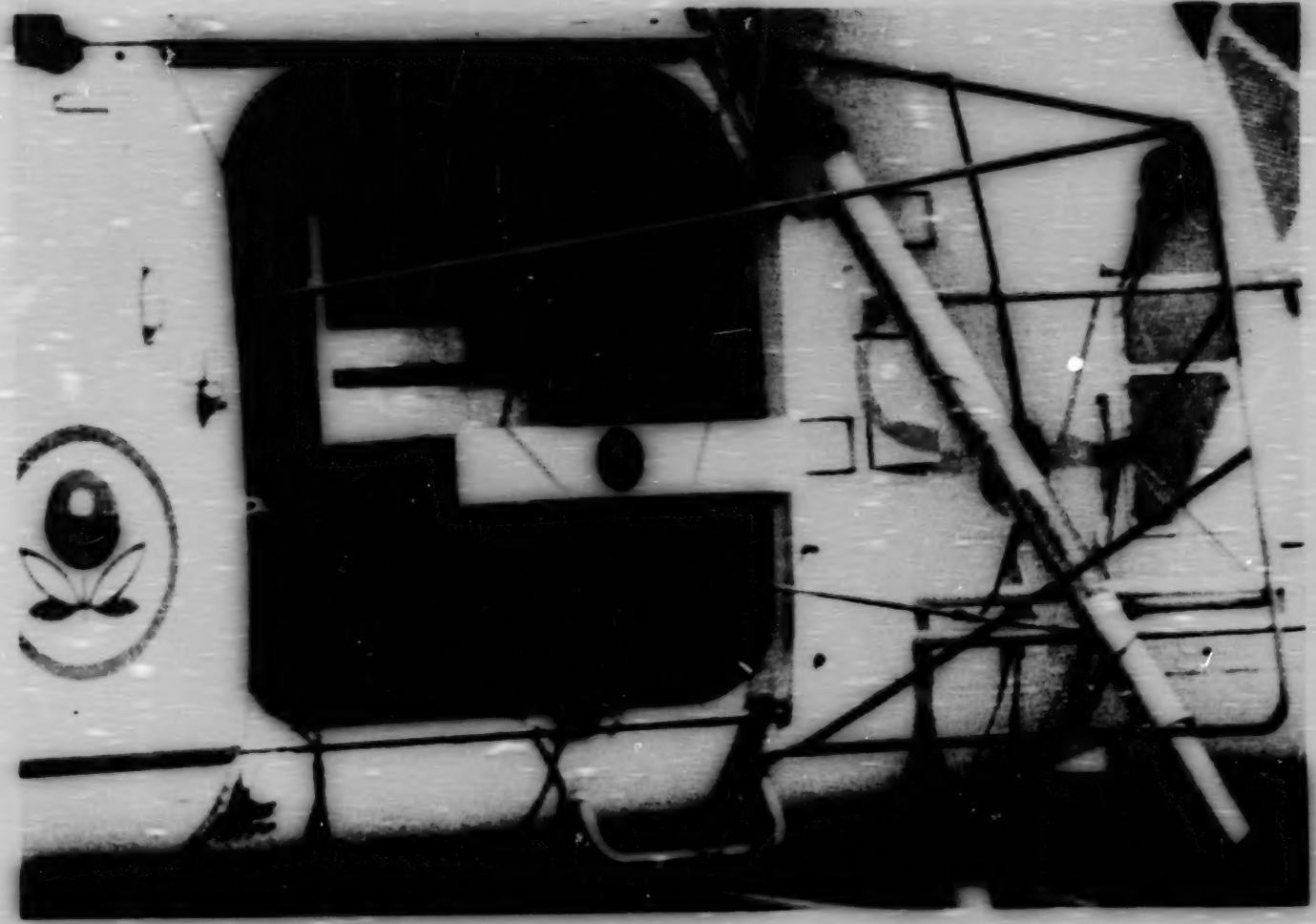

Figure 7. Optical System Installation On The EPA Helicopter.

Figure 8. PMAC 554 Signal Processing Electronics.

Digitec model 6100 and a Hewlett-Packard model 5055A. The Digitec recorder failed to operate properly during the third sampling day and was replaced with the rented Hewlett-Packard recorder. The Digitec recorder printed at a 2.5 line/sec rate while the Hewlett-Packard recorder printed at 10 lines/sec. In addition to the recorder, a Tektronix model 7633 storage oscilloscope was flown with the system in order to directly observe the signal output from the photomultiplier tube. These instruments were all strapped directly into the helicopter mounting rack for inflight use.

Figure 9 shows a block schematic of the signal processing system in front of the histogram generator. The figure illustrates how both signal visibility and time period are obtained, and the logic tests the signal must pass before it is considered acceptable for analysis. Since signal visibility was the parameter of primary interest, the following sections describe in detail how this measurement was obtained.

SDL PM VISIBILITY PROCESSOR

Spectron's approach to the measurement of fringe visibility is to use all of the information in the entire signal for the measurement. This is in contrast to other techniques (e.g., peak detection) in which the visibility is determined from only sampled portions of the signal burst. An integrator as shown in Figure 10 is a circuit which can sample a PM signal in its entirety. The integrator is turned on (i.e., starts integrating) at the beginning of the signal and is turned off at its end. If the signal is integrated directly, the periodic and random fluctuations in the signal contribute nothing to the final value of the integral. The integrator output is given by:

$$e_{out} = \frac{1}{RC} \int_0^{\tau} e_{in}\, dt \qquad (11)$$

in which e_{in} is the input voltage, τ is the integration period (i.e., the signal duration time), R is the integrator resistance, C is the integrator capacitance (RC is the integrator time constant which is of the same

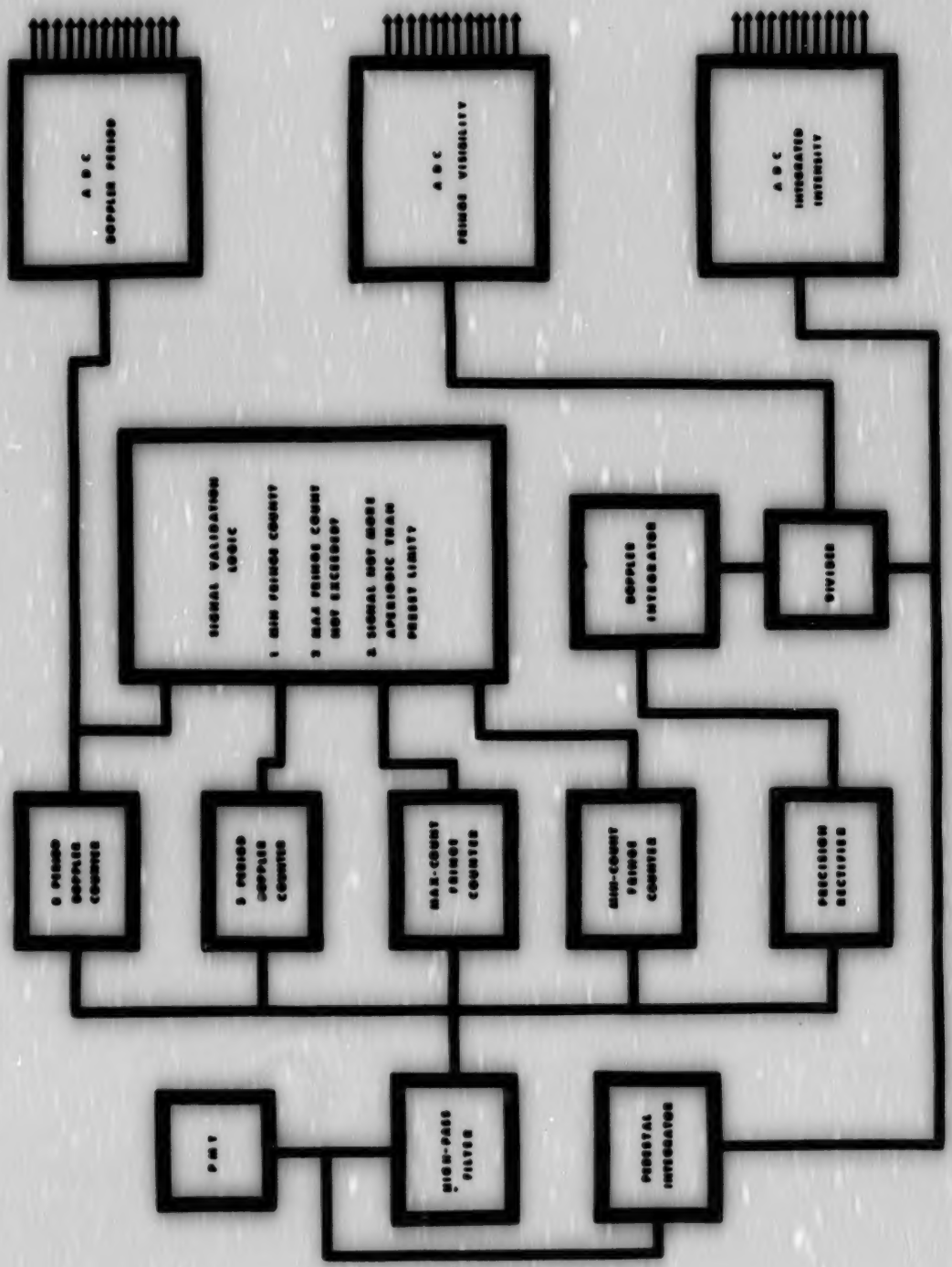

Figure 9. Block Schematic Of The Signal Processing Electronics.

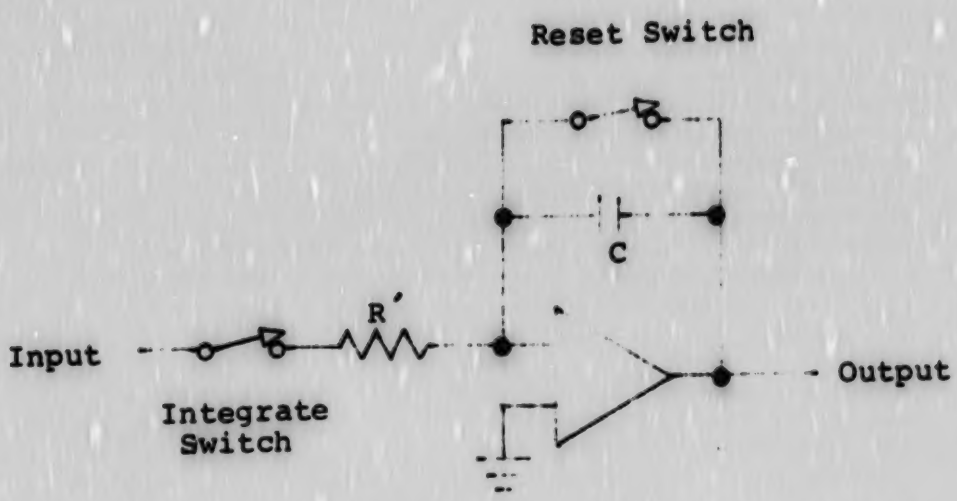

Figure 10. DC Integrator Circuit.

order of magnitude as τ), and t is time. In the visibility processor under discussion, the input signal is divided into two components. The first component is integrated directly with no further electronic manipulation. The integral of this signal approximates the integral of the DC portion of the signal. That it is not fully equivalent to the integral results from the fact that the AC component of the unaltered signal will integrate to zero only if τ is an integral multiple of the Doppler period τ_D. The circuit which turns the integrator on and off does not necessarily produce an integral time duration which is exactly an integral multiple of τ_D. Therefore, the AC component of the signal can make a contribution to the directly integrated signal. However, the time error in τ_D cannot exceed $\pm 0.5\tau_D$ and the first and last Doppler periods in the signal are small in amplitude compared to the central periods. Hence, the error in the integrator output is typically less than one percent for this integration to approximate that of the DC component of the signal that can be measured.

A second integrator is used to measure the AC component but this integrator is preceeded by two other circuits as shown in Figure 11. The DC component is first removed by a high-pass filter where the output contains only the AC component of the signal. The positive half of this signal is integrated, the negative half is inverted and then integrated, and the two integrals are summed. If the negative portions were not inverted, the two integrals would sum to zero. This design approach is electronically implemented by full-wave rectifying the high-pass filter output (which has no effect on the positive signal excursions but which inverts the negative excursions) and then integrating the rectifier output with a second integrator (see Figure 11). The output of the second integrator is a measure of the Doppler component of the signal.

The fringe visibility is obtained from the ratio of the AC integrator output to the DC integrator output.

The integration techniques outlined above have the advantage of using the entire signal for the visibility measurement. This design choice was made with belief that an averaged measurement would be more desirable than a sampled measurement in most applications. The integrators attenuate periodic and random noise sources. The basic integrator circuit shown in Figure 10 is noted for its stability and accuracy, and it is widely used in many common electronic instruments. Tables 1-3 summarize specific characteristics of the SDL PM signal processing system.

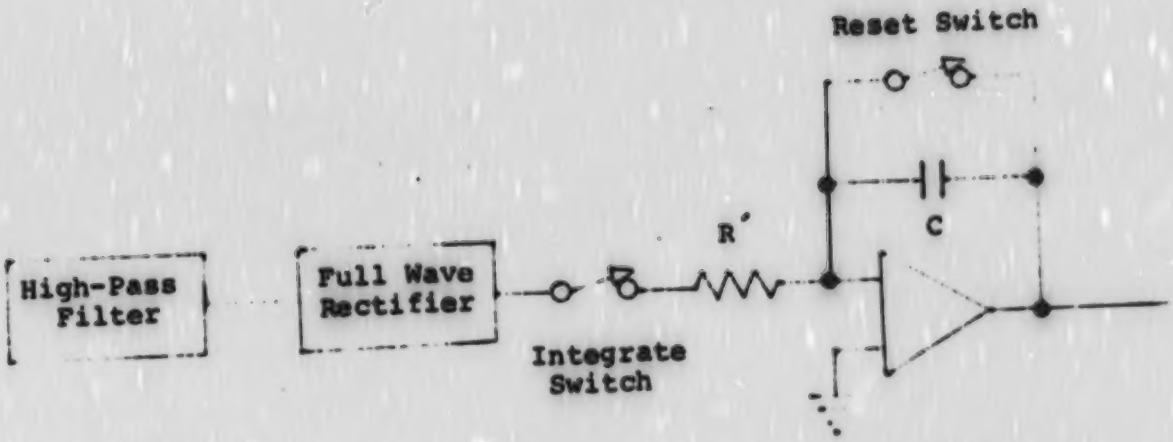

Figure 11. AC Integrator Circuit.

Table 1. DOPPLER PERIOD PROCESSOR

Frequency Response (various channel carrier frequencies available on request)	0 - 10 MHz
Time Period Resolution:	3 Digit BCD
Time Period Accuracy:	Nominal 1%
Bandpass Filter Ranges:	0.5 KHz, 1.0 KHz, 2 KHz, 5 KHz, 10 KHz, 20 KHz, 50 KHz, 100 KHz, 200 KHz, 500 KHz
Integrated Signal Amplitude Dynamic Range:	10^4
Maximum Data Acquisition	20,000 sec^{-1}
Minimum Signal Input Amplitude	10 millivolts
Data Output Code	Analog, 12 Bit BCD and Binary. TTL Compatible
Error Logic	• Programmable Periodicity Ratio Check • Programmable Aperiodicity Acceptance Error • Min/Max Cycle Count • Programmable Periodic Signal Sampling
Processor Operating Voltage	110v/60 Hz

Table 2. VISIBILITY PROCESSOR

Frequency Response (various channel carrier frequencies available on request)	0 - 2 MHz
Visibility Range	1.0 - 0.1
Visibility Resolution	± 0.1%
Visibility Accuracy	± 0.1%
Equivalent Possible Spherical Particle Size Range	15:1
Signal Amplitude Dynamic Range	10^4
Maximum Data Acquisition Rate	20,000 sec^{-1}
Minimum Signal Input Amplitude	10 millivolts
Data Output Code	Analog, 12 Bit BCD and Binary. TTL Compatible
Error Logic	• Programmable Periodicity Ratio Check • Programmable Aperiodicity Acceptance Error • Min/Max Cycle Count • Programmable Periodic Signal Sampling
Processor Operating Voltage	110v/60 Hz

Table 3. HISTOGRAM GENERATOR

- Forms Histograms of:
  - Signal Visibility
  - Signal Time Period
- 15 Bins
- Bin Width Programmable.
- Four Data Normalization Modes
  - Total Histogram Signal Count For Preset Count Number (10, 10^2, 10^3, 10^4)
  - Total Signal Count For Most Frequently Occupied Histogram Bin For Preset Count Number (10, 10^2, 10^3, 10^4)
  - Total Event Count For Preset Count Number (10, 10^2, 10^3, 10^4)
  - Periodic Histograms For Preset Sample Time (10/sec.- 0.01/sec.)
- Total Number of Events Display
- Number of Measurements in Histogram Memory Display.
- Total Signal Count Timer
- Nominal Maximum Memory Fill Rate 50,000 sec^{-1}
- Data Output Code: BCD TTL Compatible (Binary, Analog Optional)

SECTION VII

RESULTS

The following is a presentation of the results obtained with the PM system during the data acquisition flights and specific flight tests for the instrument. The data is identified by the date and particular flight on which it was recorded.

Since there was no provision made for an automatic time record of the data acquisition times for the PM system and any other instruments used for the inflight samples, only rough estimates of where a particular sample was obtained during the flight can be made. The inflight operator kept notes of facts pertinent to the condition under which a particular data set was obtained. These notes were recorded on the digital recorder printout, and are summarized in the tables for each day's flights. The daily log given in Appendix A indicates why the instrument could not acquire data on the days for which it is lacking.

NOVEMBER 19 / TEST FLIGHT

The first flight for operating the PM system was a test flight to determine its airborne operating characteristics. Particular attention was paid to environmental effects (e.g., aircraft vibration and sunlight) on the operating characteristics of the system. The data samples obtained with the system were in the Chandler area near an agricultural region that was at the edge of the desert. A number of passes were made at different altitudes and through dust raised by agriculture equipment operating on fields freshly prepared for planting.

Background sunlight was observed to present some problem when the zenith angle of the sun with respect to the optical transmission axis was less than about 45°. A technique which appeared to significantly reduce the background light was to limit the instrument operation to times when the door of the aircraft pointed away from the sun. With the exception of the digital recorder, the instrument appeared to function well in all respects. The digital recorder printed the histogram results in such a manner that it did not consistently print the "10" column digits, and occasionally did not print digits in the other columns. It was usually found that the digits were not printed if they were zeros.

Thus, the particle size distribution data obtained is subject to broad error bands when the "10" column was uncertain and the number of measurements small. It was possible, however, to estimate the most frequently occurring particle size. Table 4 provides a summary of this kind of data for flights over a series of grass covered fields which were bounded on one side by an occasionally travelled unpaved roadway. As Table 4 shows, the particle size mode follows the trend that might be expected for particle size variation with altitude. Figures 12 and 13 show an example of the particle size distribution obtained during a 30 m pass over freshly prepared fields at approximately 1700 hours. The distribution contained sufficient counts such that a reasonably accurate size distribution could be obtained. The standard deviation for this distribution is surprisingly small for what might have been expected under the circumstances. The skewness shown by the histogram in Figure 12 is what might be expected for a crushed powder and is therefore reasonable. A second interpretation of the data suggests that there are two sources for large particles - paved and unpaved roads. The paved roads should yield a broader size distribution with a smaller mean size due to the crushing action of tires on the hard surface. The unpaved roads should yield distributions with larger mean sizes due to the stirring action of tires passing along the road bed. The deviation of the data points about the straight line on the accumulative probability plot is believed to be due to the uncertainty resulting from the missing "10" column due to erratic recorder operation.

NOVEMBER 22 / DATA ACQUISITION FLIGHTS

Two missions were flown on November 22. Preflight tests on the ground indicated potentially high noise levels due to background sunlight. However, it was decided to fly the system with the operator choosing the operation sequences for minimum sunlight levels. After the system was airborne, the signal threshold level was optimized to a value of about 7 and reduced to smaller values for the late afternoon flight. Tables 5 and 6 summarize the data obtained during these flights.

The data obtained during the first flight showed the unexpected result of a single bin being populated in 20 - 25 μm range. This occurred with varying numbers for the first 6 histograms. Such a count configuration was not observed thereafter. The count configuration is not indicative of system noise (which would tend to fill the largest particle size bins). There is no reason to suspect an instrument malfunction for this data, although the fact that nearly all the measurements are contained in a single bin makes the data somewhat questionable.

Table 4. MOST FREQUENTLY OCCURRING PARTICLE SIZE AS A FUNCTION OF ALTITUDE FOR 1600 HOURS, NOVEMBER 19, 1975

Altitude (m, AGL*)	Altitude (ft. AGL)	Particle Size (μm)
152.4	500	40 - 45
91.4	300	55 - 60
30.5	100	65 - 70

*Note that the term "AGL" references altitude relative to altitude "above ground level".

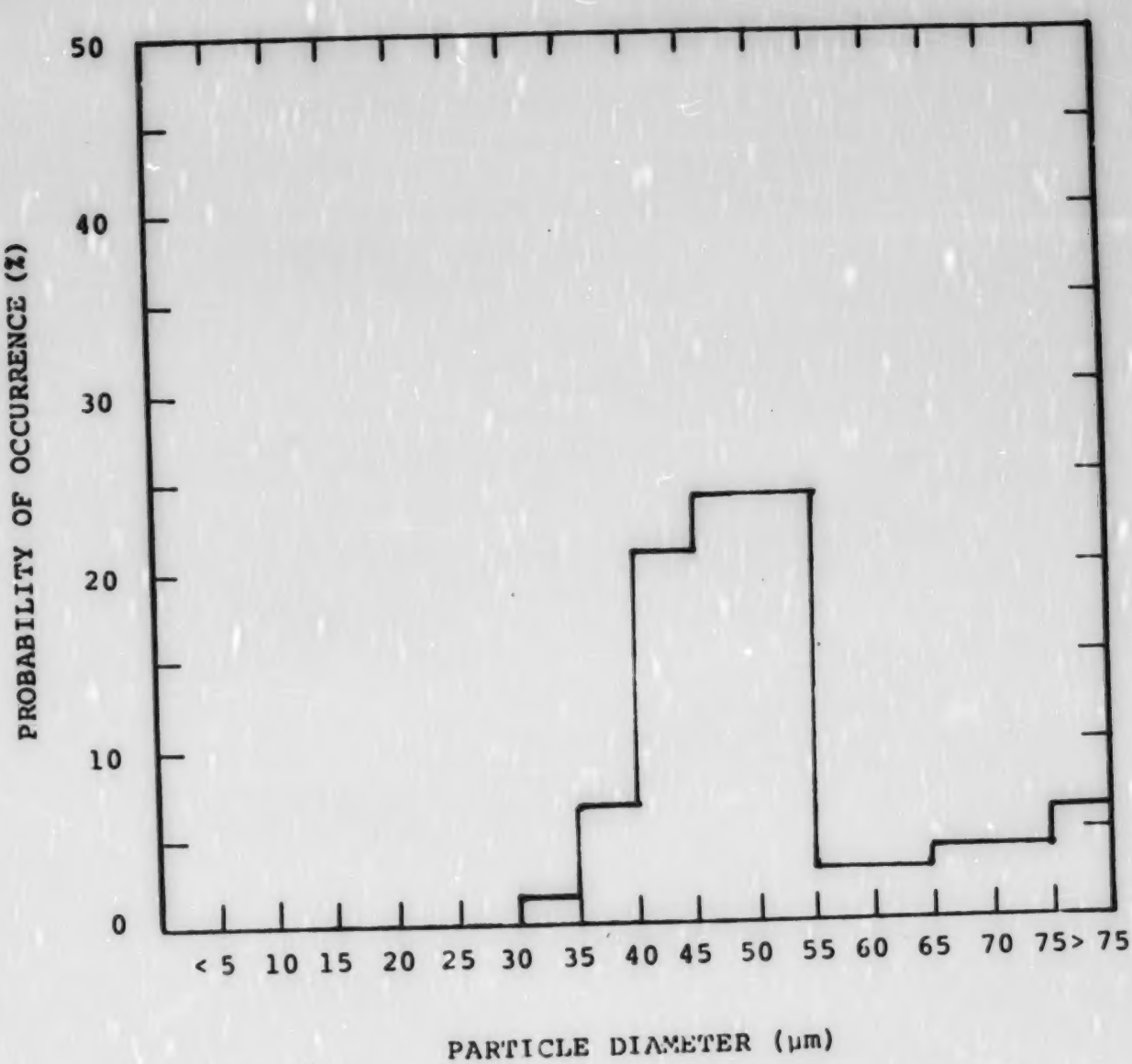

Figure 12. November 19. Histogram From Instrumentation Test Flight @ 30.5 m AGL In Chandler Area.

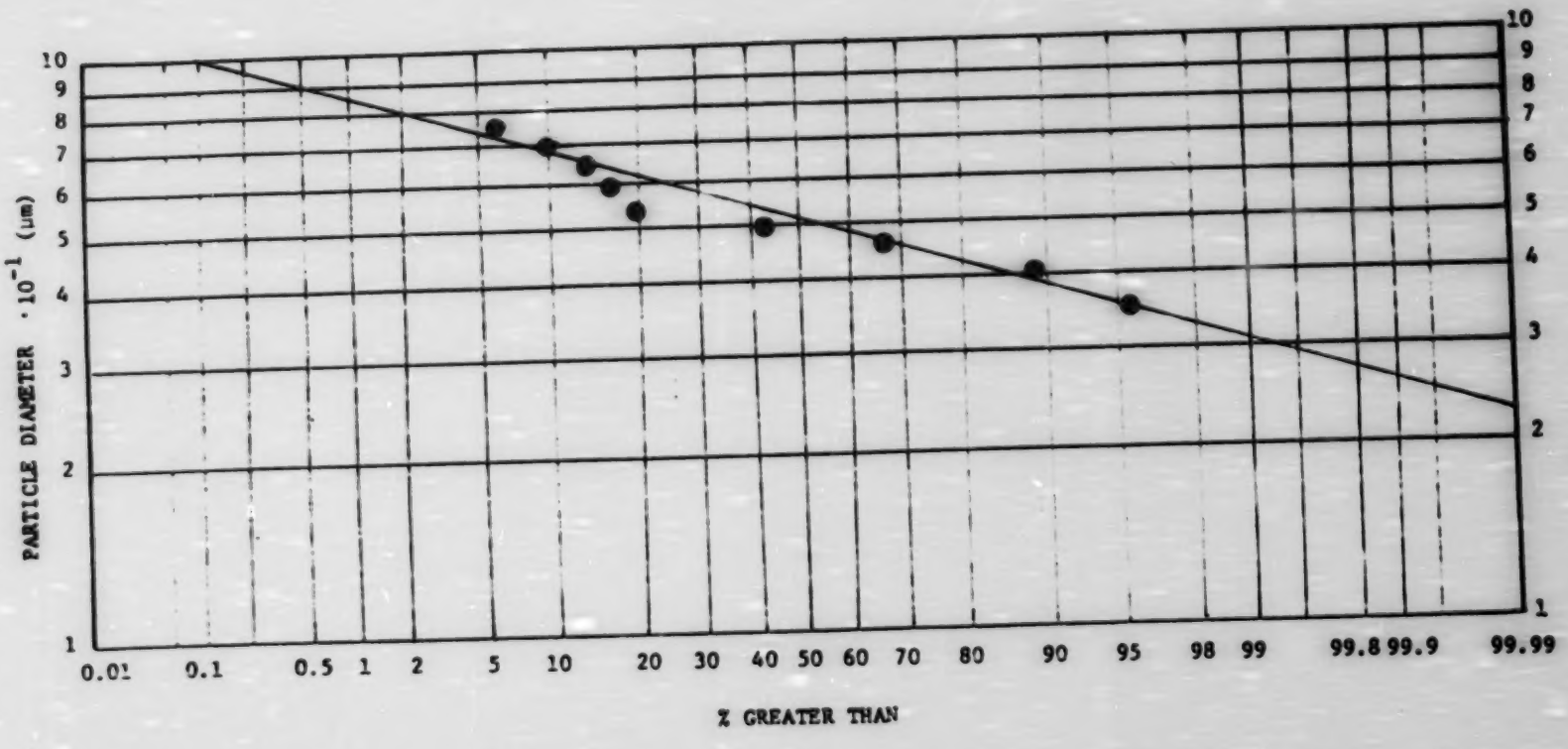

Figure 13. November 19, particle size distribution obtained during instrument test operation flight in the Chandler area. 30.5 m AGL altitude with approximate data rate of 200 measurements/sec.

Table 5. NOVEMBER 22, FLIGHT 1. PM SYSTEM DATA SUMMARY

Histogram Number	Track	Altitude (meters AGL)	Flight Notes
1	?*	30.5	7.4 Threshold
2	?*	30.5	Stray Laser Light Due to Pull-In Strap For Filter Holder
3	?*	30.5	
4	?*	30.5	
5	?*	30.5	
6	?*	30.5	
7	?*	30.5	
8	?*	30.5	(2) 30 Sec. Auto Sequences

*Flight notes do not indicate tracks for which data was obtained.

Table 6. NOVEMBER 22, FLIGHT 2. PM SYSTEM DATA SUMMARY

Histogram Number	Track	Altitude (Meters AGL)	Flight Notes
1	?*	30.5	High Sun Level
2	?*	30.5	High Sun Level
3	?*	30.5	5.0 Threshold
4	?*	?**	Dust Mission
5	?*	?**	4.3 Threshold
6	?*	?**	
7	?*	?**	3.8 Threshold
8	?*	?**	
9	?*	?**	
10	?*	?**	Ground Test

*Flight notes do not indicate tracks for which data was obtained.

**No altitude indication on digital recorder data.

Figure 14 is the "reduced" particle size histogram obtained from histogram 7. The term "reduced" is used to describe the fact that the histogram was normalized with the counts in the 20 -25 μm bin removed. Even with the counts for the 20 - 25 μm bin removed, the distribution is clearly multimodal. The data seems to show distinct mode sizes at 20 - 25 μm, 55 - 60 μm and somewhat greater than 75 μm. However, the unreduced histogram has 96% of the measurements concentrated in the 20 - 25 μm bin.

During the second flight, a very low percentage of measurements were recorded in the 20 - 25 μm bin (typically less than 4%). The large majority of the measurements were recorded in the greater than 75 μm bin. However, immediately upon landing (1800 hours) a particle size histogram was obtained for the ground level distribution. Figure 15 shows the results of that set of measurements. Three mode sizes 25 - 30, 50 - 55, and greater than 75 μm are apparent.

NOVEMBER 23, 24 / DATA ACQUISITION FLIGHTS

Two flights were flown during the evening of November 23 and early morning of November 24 before sunrise. The first flight began at about 2230 hours on November 23 and terminated at about 0030 hours November 24. The second flight began at 0400 hours November 24 and terminated at 0600 hours. The atmosphere was exceptionally clear and the data acquisition rate low. For example, on November 19, the data rate had been between 10 and 200 measurements per second. During the track measurements on the 23 and 24, the data acquisition rate varied from 0.25 per second to less than 0.1 per second. Tables 7 and 8 summarize the data acquired during the flights.

The first two histogram sequences during the first flight were for 30 second automatic sequence times. It became apparent that at the 366 m altitude, the particle density was too low to record any measurements in the sample time. Hence, the instrument was placed in a manual operational mode and only one histogram attempted per flight track. Nearly all the particle sizes observed were greater than 60 micrometers in diameter. Figures 16 - 18 are histograms for the particle sizes observed during these flights. The data was deemed to be too sparse for accumulative probability plots which could provide statistical information on the data so obtained. However, it is interesting to observe that the distribution mode appears to shift toward smaller sizes as the altitude is increased.

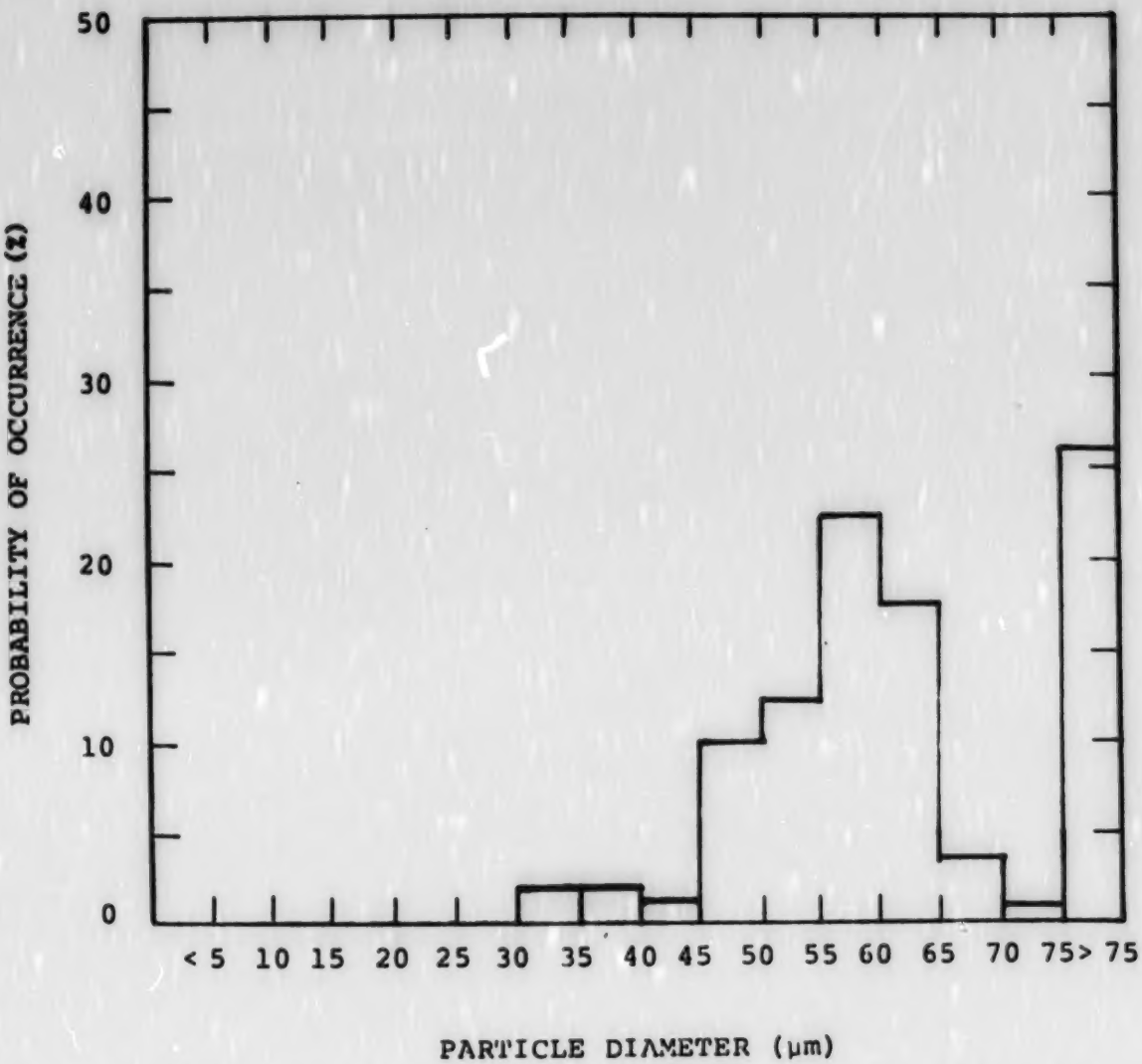

Figure 14. November 22. Histogram 7, Flight 1. Particle Size Distribution.

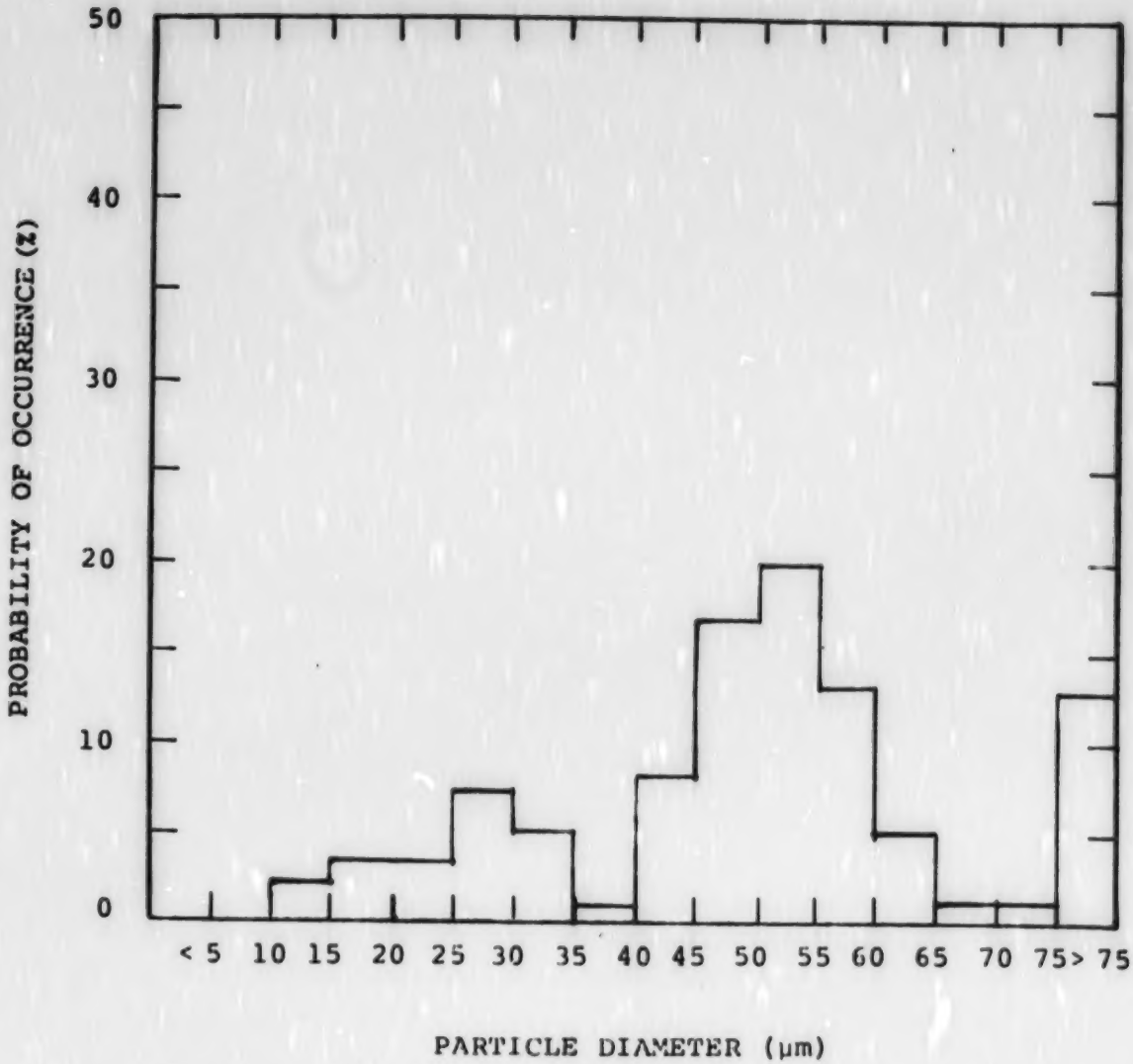

Figure 15. November 22. Ground Test After Second Flight. Particle Size Distribution.

Table 7. NOVEMBER 24, FLIGHT 1. PM SYSTEM SUMMARY

Histogram Number	Track	Altitude (Meters AGL)	Flight Notes
1	10	366	(1) 30 Sec. Histogram
2	10	366	30 Sec. Autosequence
3	10	366	Histogram Acquisition Time: 2318 - 2335
4	4	152	Histogram Acquisition Time: 2348 - 0005
5	4	366	East Bound. Histogram Acquisition Time: 0007 - 0025
6	4	366	Velocity Histogram

Table 8. NOVEMBER 24, FLIGHT 2. PM SYSTEM DATA SUMMARY

Histogram Number	Track	Altitude (Meters AGL)	Flight Notes
1	9	366	Threshold Test @ 4.5
2	9	152	Threshold Test @ 5.0
3	9	152	Threshold Test @ 4.5 (very low data rate)
4	Flight To Track 3		
5		366	
6	3	366	
7	3	152	
8	Return To Airport From 366 meters	76	10 Second Autosequence

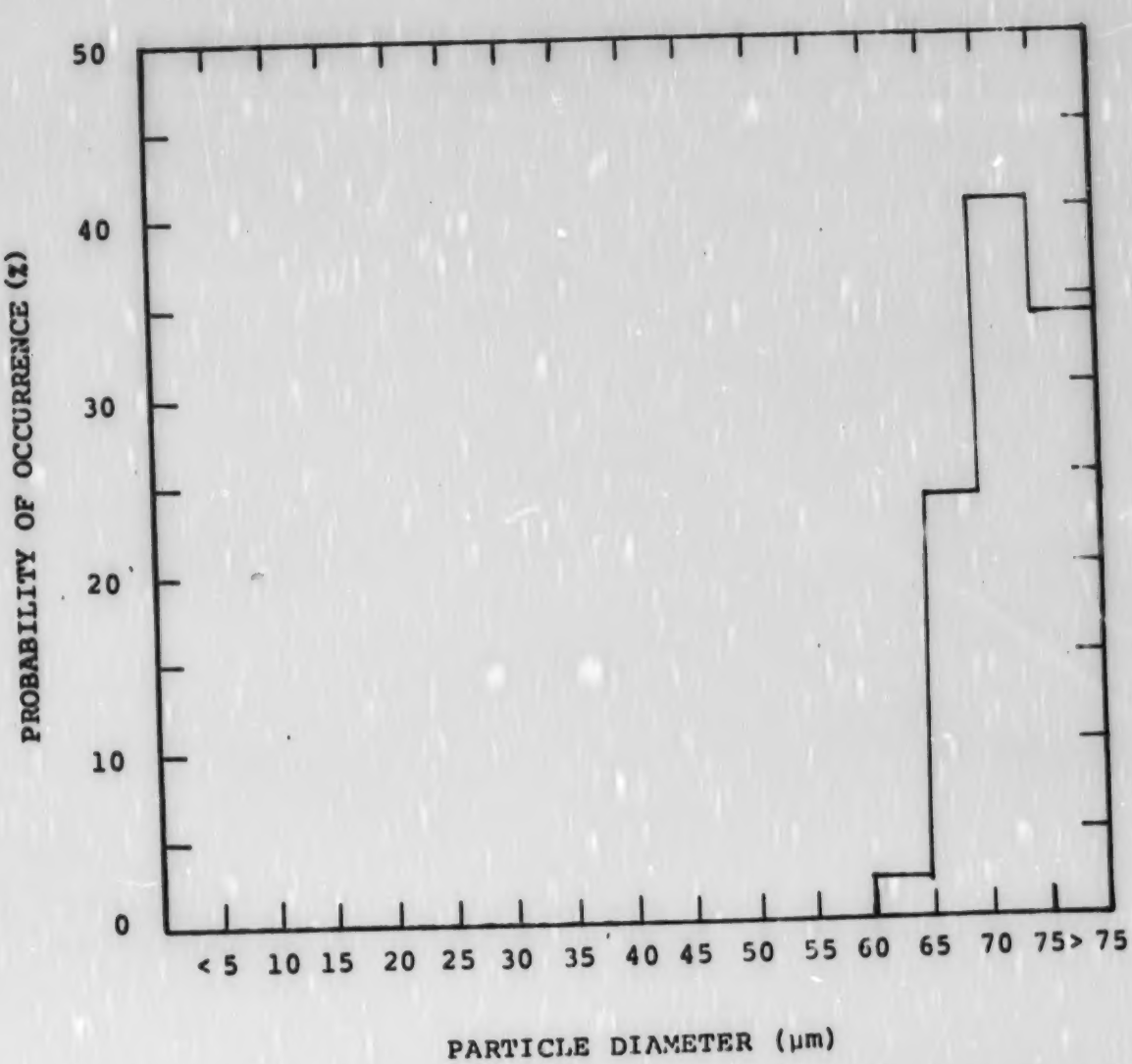

Figure 16. November 24. Histogram 3, Flight 1. Particle Size Distribution.

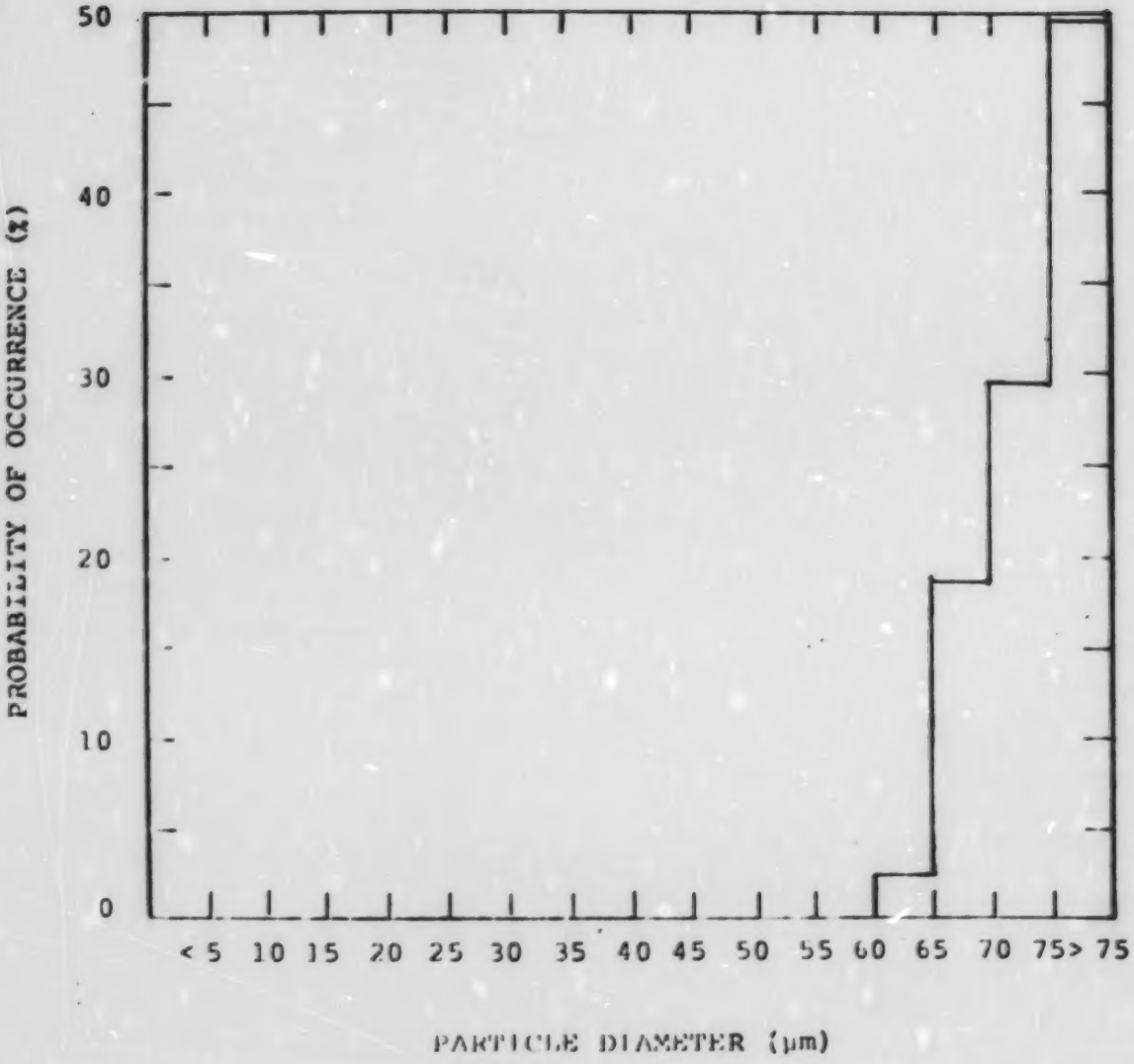

Figure 17. November 24. Histogram 4, Flight 1. Particle Size Distribution.

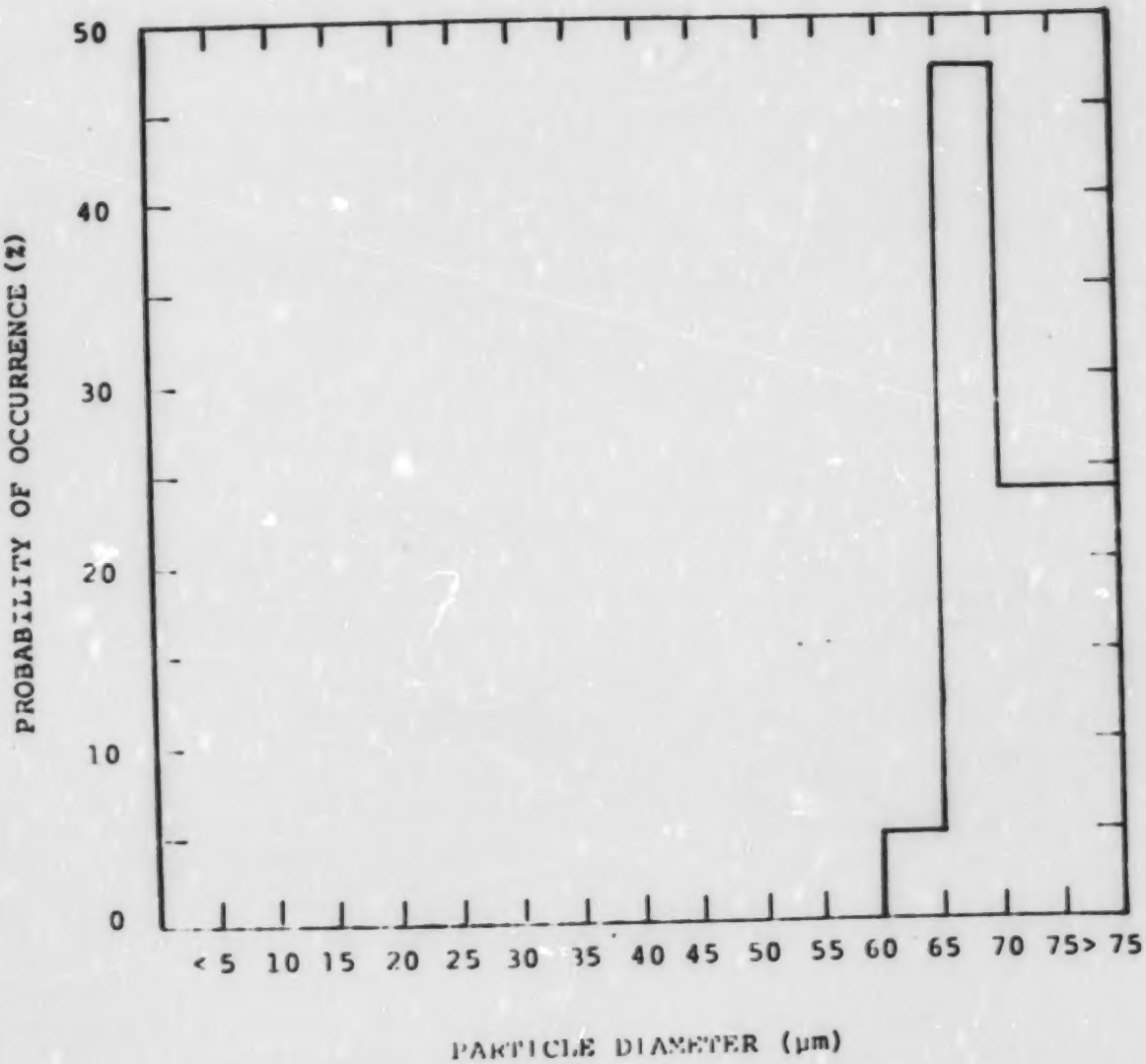

Figure 18. November 24. Histogram 2, Flight 1. Particle Size Distribution.

Near the end of the flight on track 4, a velocity histogram was obtained. The measurements were for a sample space which set 51 cm (20.25") from the edge of the optics cabinet. The results are shown in Figure 19 as an accumulative probability plot of the signal time period. The figure shows that the mean velocity was 12.5 ± 4.9 m/sec., which is considerably less than the helicopter air speed of approximately 41 m/sec. The signal time period distribution shows that the flow through the sample space was quite turbulent. It should be borne in mind that the velocity component measured is that parallel to the centerline of the aircraft, and that the sample space of the instrument could still be well within the boundary layer of the aircraft, or shadowed by the wheel strut.

Due to the exceptionally low data rate, it was decided to vary the signal level threshold during the second flight in order to determine if the instrument was possibly rejecting signals with too low an amplitude. There was no measurable difference between the low and high values of the instrument threshold settings. This indicated that the particle number density was extremely low as the first flight had indicated. Over 95% of the measurements obtained in the histograms during this flight were predominately located in the bin containing sizes greater than 75 micrometers. The data rate was typically less than 0.8/sec.

Upon return to the airport, the PM was set to automatically obtain a histogram sample once every 10 seconds as the aircraft descended from an altitude of 366 m. Descent rate was 1.27 m/sec, so that a sample of the relative number density over 12.7 m intervals was obtained. The PM did not operate while the digital recorder recorded the histogram. Thus, there are 2 m intervals where no sample was obtained while the recorder functioned. Figure 20 shows that measured relative number density as a function of altitude. It is clear that the number density is not isotropic with altitude. The figure shows variations of factors of 2 or 3 in 25 m altitude changes. The figure shows an exceptionally high number density below an altitude of about 28 m which is believed to be indicative of the inversion layer. The data for the last 14 m of altitude suggests that the PM is observing particles swept up from the ground by the aircraft downwash. This conclusion follows by examining the particle size distributions for these altitudes and comparing them with a distribution obtained approximately 10 minutes after landing. An accurate estimate of absolute number density is not possible since the size of the sample space cross-section was not calibrated. However, a rough estimate of the cross-sectional area can be made predicated on previous water spray calibration measurements. For a 500 μm slit aperture width, the absolute number density ρ is roughly approximated as:

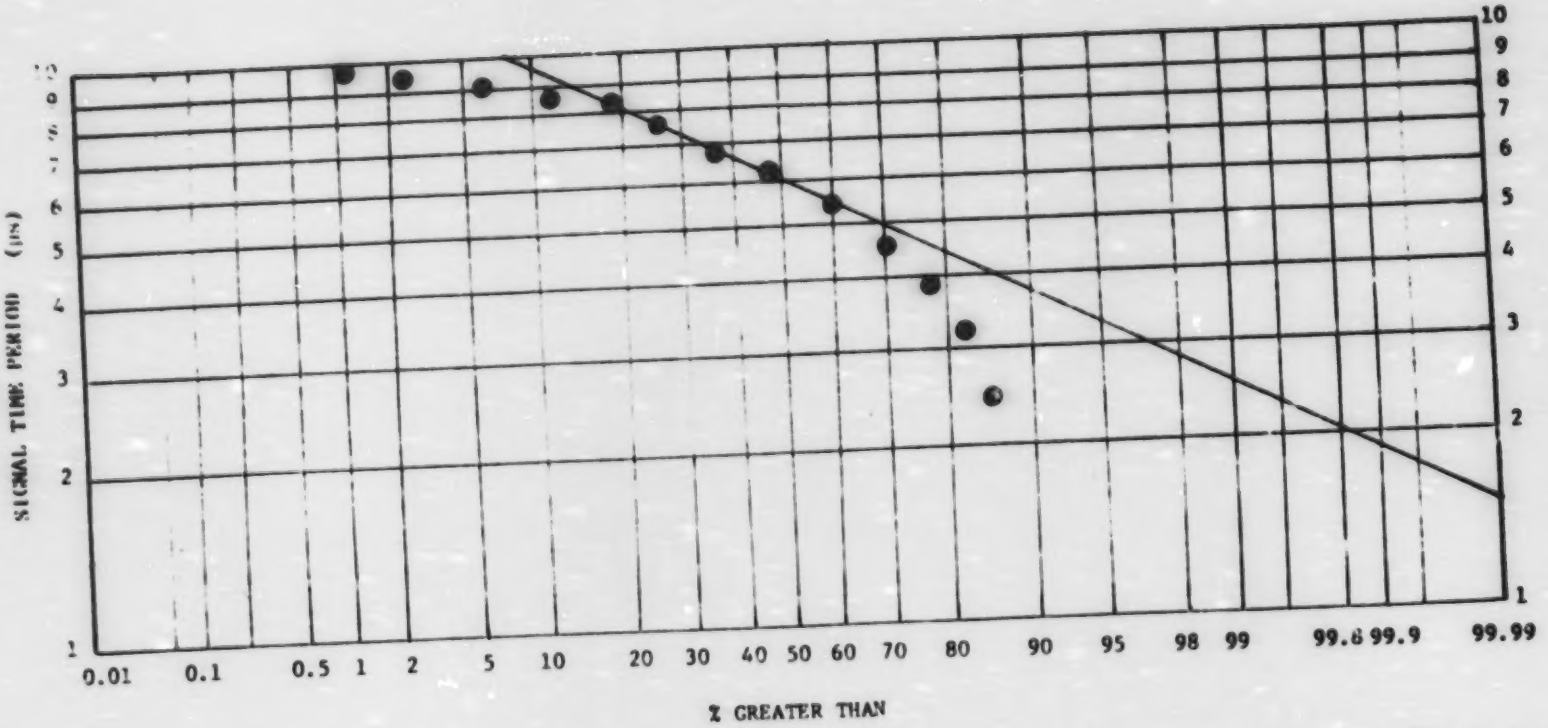

Figure 19. Signal time period distribution for velocity determination. Obtained 0025 hours November 24, East bound, 366 m AGL.

Figure 20. November 24, Flight 2. Return to airport. Descent from 366 m AGL altitude at 76 m/min. rate. Relative number density distribution over 12.7 m altitude increment for a vertical sample path.

Reproduced from best available copy.

$$\rho = \dot{N}/vA \tag{12}$$

$$\rho = 2.9.10^{-3}\dot{N}\ cc^{-1} \tag{13}$$

where v is the sample space velocity, A is the sample space cross-sectional area and $\dot{N}$ is the number of observed signals per second. The assumed numerical value of A is purely a guess predicted on the observed length-to-width ratio observed in water spray calibrations. It is expected to be within a factor of 2 or 3 of the true value.

Figure 21 shows that the mode for the size distribution is between 70 and 75 micrometers for the altitude increment lying between 27.9 and 15.2 m. However, Figure 22 shows that particle size mode is greater than 75 μm in the altitude increment nearest the ground. Comparison of these two distributions with that of Figure 23 indicates the 27.9 - 15.2 m altitude distribution is very similar to that of the undisturbed atmosphere at ground level. Since the previous flight data showed that the PM sample space velocity is approximately 1/3 that of the aircraft, it would appear entirely possible that the sample at the 14 to 1.3 meter altitude reflects the ground level dust stirred into the aircraft airstream by the rotor downwash. The above conclusions, however, are not definitive since there is an approximate +12.7 m, -0, uncertainty in altitude which resulted from the way the automatic sequence was terminated. Figure 20 was constructed under the assumption that the automatic sequence was terminated immediately after the last histogram was recorded.

NOVEMBER 25 / DATA ACQUISITION FLIGHTS

The flights for November 25 began at approximately 0700 and 1030 hours respectively and were about two hours in duration. During these flights, a second background light filter was used giving an estimated passband of 70 nanometers. This reduced the scattered light amplitude to the photodetector but allowed the use of increased amplifier gain. To further compensate for the reduced instrument transmission, the lenses in the optical system were adjusted to move the sample to a position 28.5 cm (11.25 inches) from the optics cabinet. The same fringe period used at the 51.4 cm (20.25 inches) position was maintained. At this position, the sample space appeared to be nearly shadowed by the aircraft wheel strut. Furthermore, since the sample space was moved closer to the

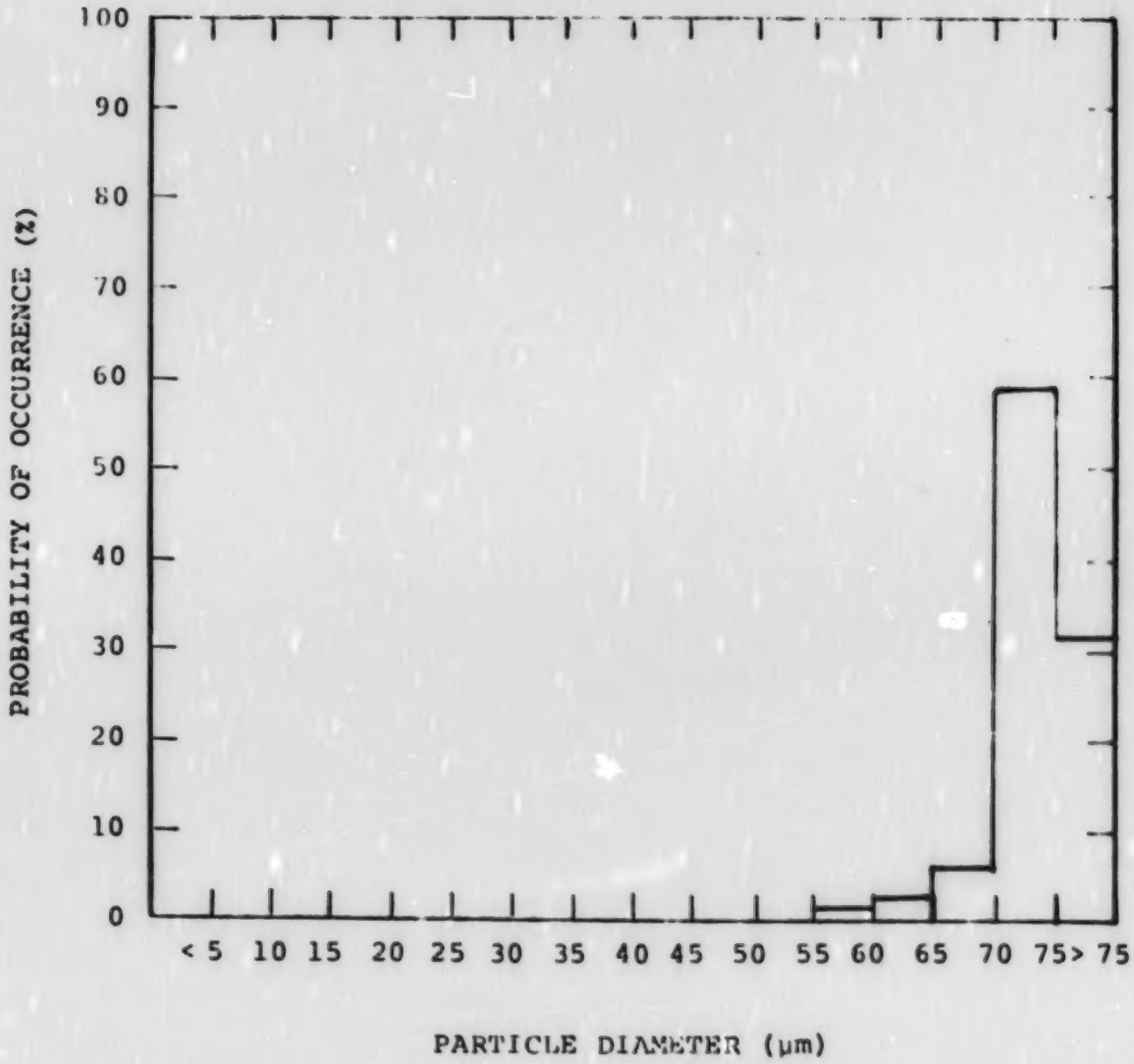

Figure 21. November 24, 0600 hours. Inversion Layer Histogram For 27.9 - 15.2 m Altitude Increment. Particle Size Distribution.

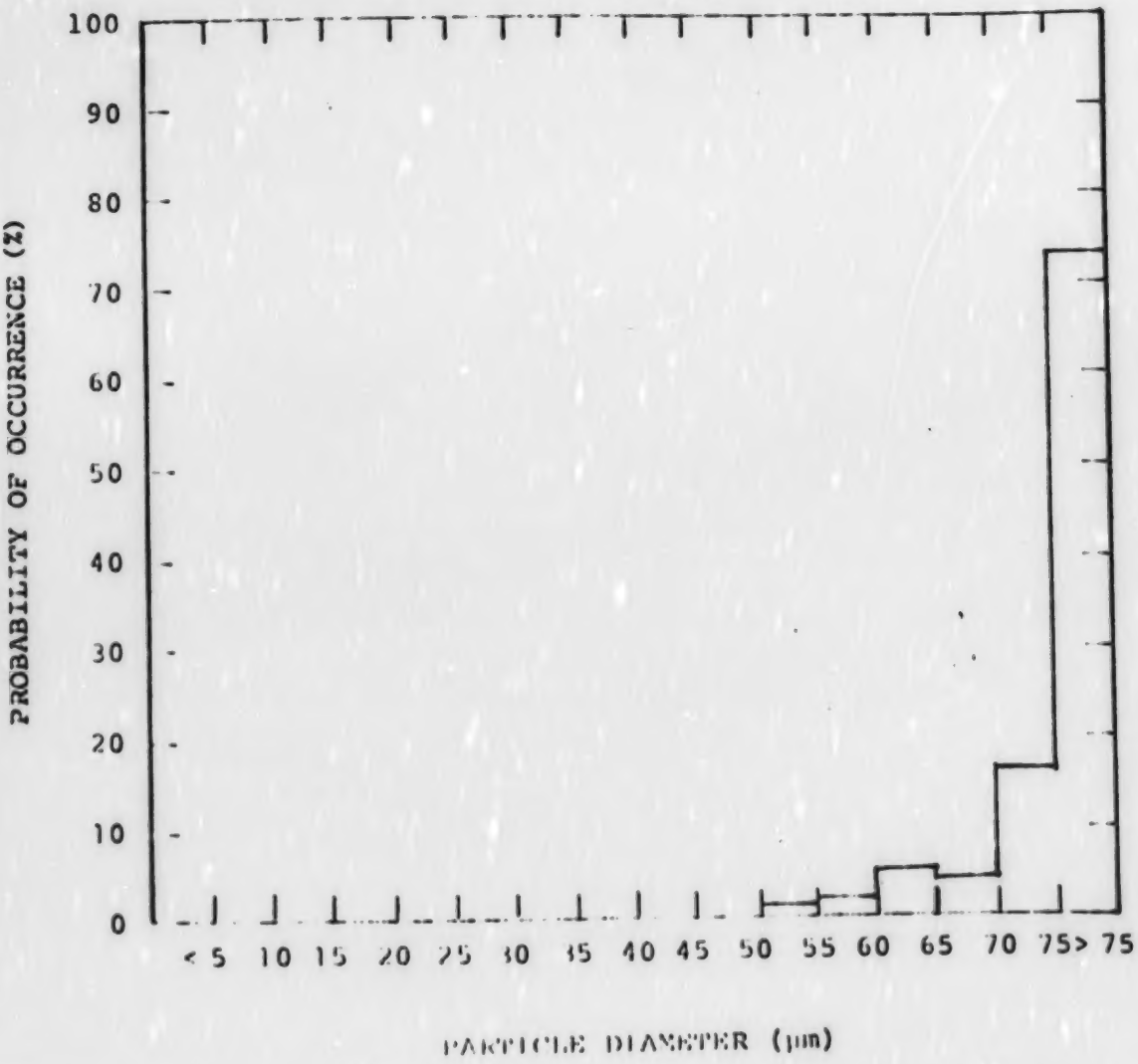

Figure 22. November 24, 0600 hours. Inversion Layer Histogram For 13.9 - 1.3 m Altitude Increment. Particle Size Distribution.

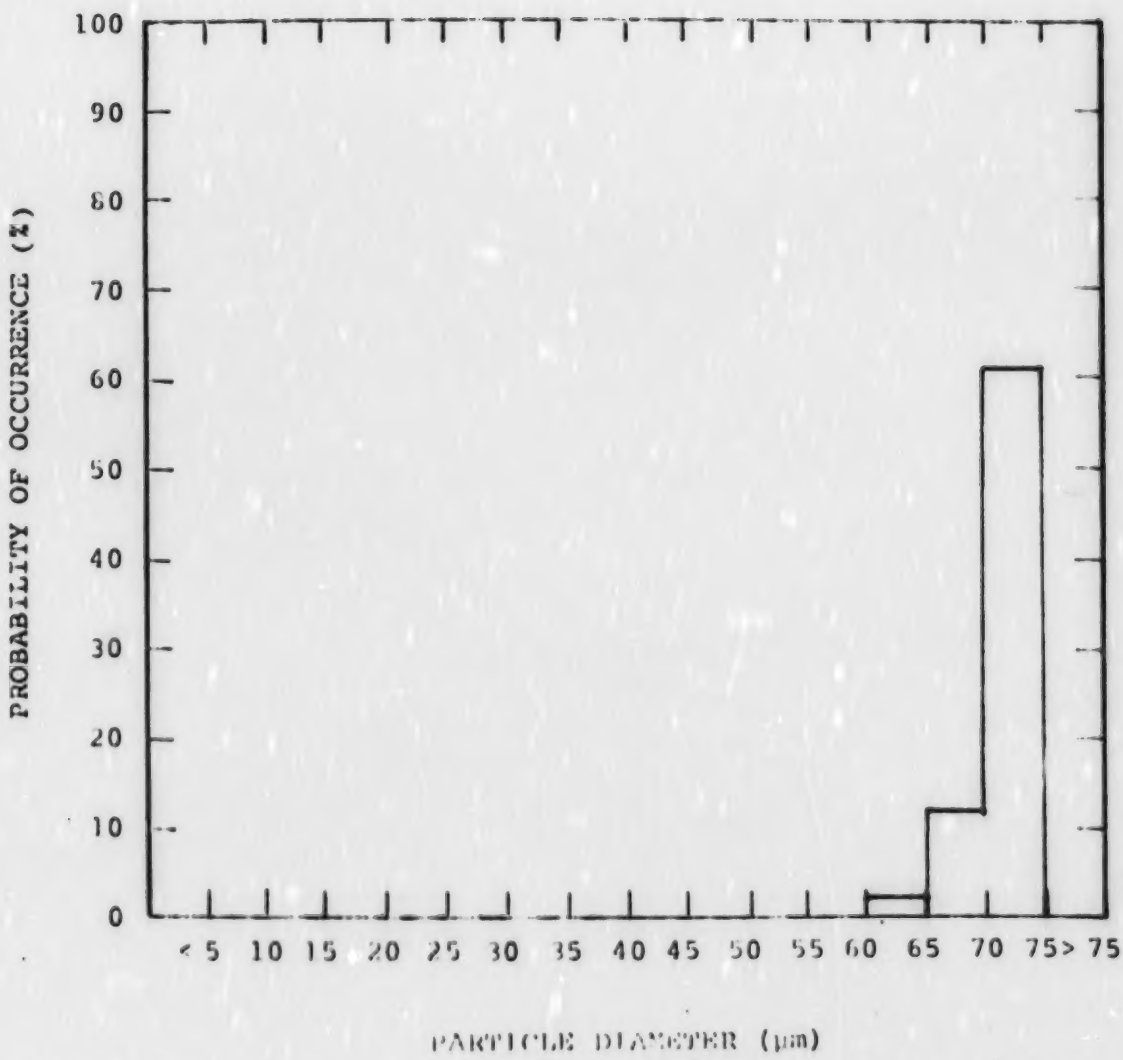

Figure 23. November 24. Ground Based Measurement Immediately After First Flight. Particle Size Distribution.

aircraft, it is to be expected that the air velocity should be less than at the previous sample space position. As the data shows, this expectation was confirmed. Figure 24 is an accumulative probability plot of the signal time period distribution obtained during the second flight. The mean time period indicates a velocity of 9.6 ± 4 m/sec. Comparison with the velocity measurement at the previous sample space indicates that the turbulence level was increased (probably because of the wheel strut).

Table 9 summarizes the status of the histograms obtained during the first flight. A programming error was made in the PM preflight setup which caused all measurements of particles greater than 75 micrometers not to be entered into memory. As a result, the distributions are somewhat skewed. This error was corrected for the second flight. During the second flight, it was found that a relatively small percentage of the size distribution occurred for sizes greater than 75 μm, so that this error for the first flight had little effect on the overall results. Figure 25 presents the results of histograms 1 - 4 in terms of accumulative probability plots. Figures 26 - 29 are the corresponding histograms. The distributions are characterized by mean sizes between 68 and 72 μm, and relatively small standard deviations. The data for histograms 5 - 7 was obtained for the most part in an auto-sequence mode, and predominately contains measurements in the 70 - 75 μm size interval. Data from the last track east of Phoenix for the first flight is given in Figures 30 -32. These data suggest that while the mean particle size remains approximately constant, the standard deviation of the distribution has increased. In fact, the data indicated measurements across the entire size range although the frequency of occurrence was very small compared to that for sizes generally greater than 60 μm. It was interesting, therefore, to examine the relative distribution of these measurements with the larger sizes removed. Figures 33 - 35 show the results of artificially modifying histograms 7 - 9 by removing the populous larger size bins. Since these distributions represent only about 100 total measurements each, very little can be said about the distributions they might represent. It is interesting to note, however, that there appear to be distinct size modes occurring between 5 - 10 μm and 15 - 30 μm as shown in Figures 34 and 35 respectively.

Data obtained during the second flight is summarized in Table 10. Data obtained in the first two histograms was obtained during signal level threshold adjustments. The originally set threshold was adjusted downward to give the instrument increased sensitivity after it was observed that background light did not appear to interfere with the measurement at the lower threshold setting. The data from the first two histograms

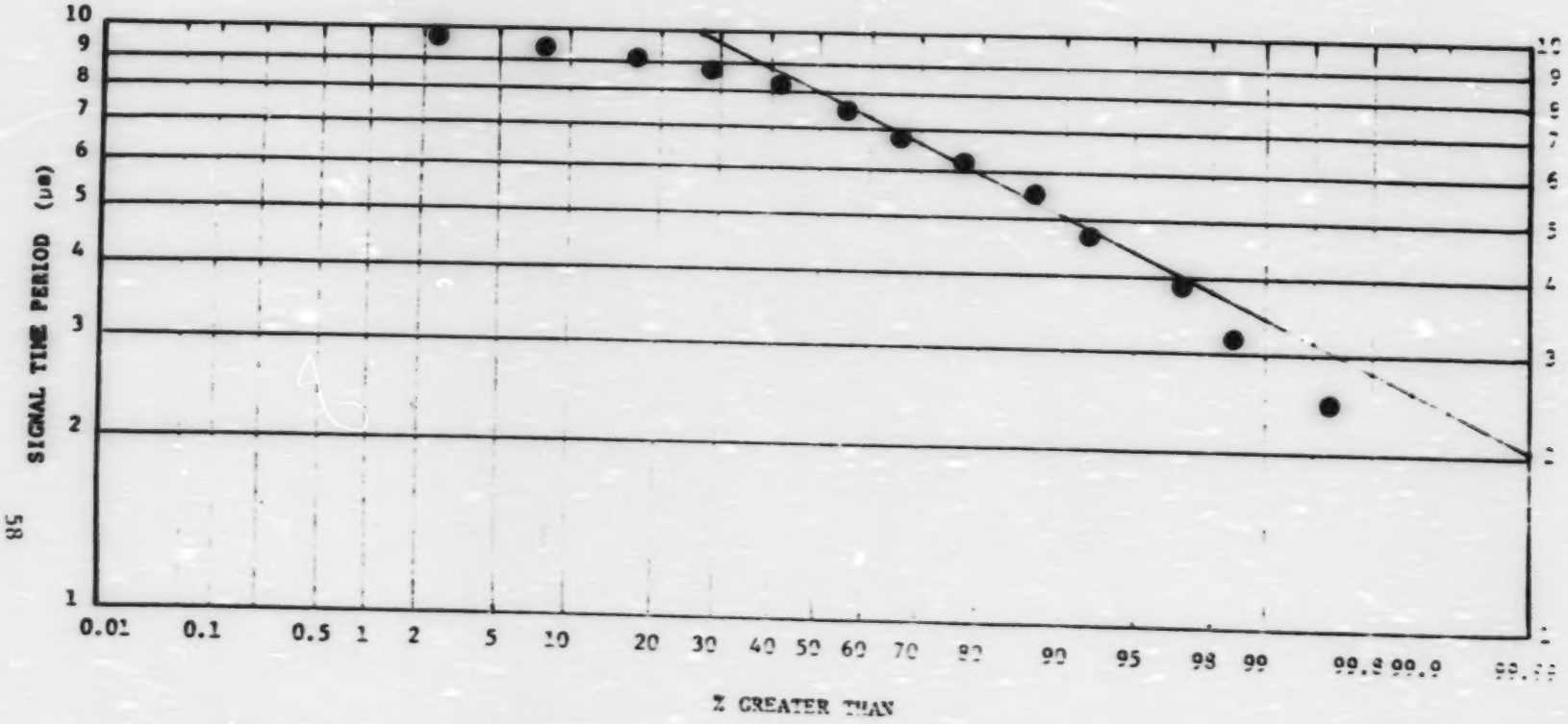

Figure 24. November 25, Flight 2. Signal time period distribution for velocity determination.

Table 9. NOVEMBER 25, FLIGHT 1. PM SYSTEM DATA SUMMARY

Histogram Number	Track	Altitude (Meters AGL)	Flight Notes
1	11	152	Flight Notes Are Sparse. Data Sequence Suggests That Histograms 2 & 3 Are Also At 152 meters Track 11.
2	*	**	
3	*	**	
4	*	**	
5	*	30.5	11.5 Miles South Of Phoenix VOR
6	*	**	
7	*	30.5	30 Sec. Autosequence
8	*	30.5	8 & 9 Are Last Run On East Side of City
9	*	30.5	

*No Track Indication On Digital Recorder Data.

**No Altitude Indication On Digital Recorda Data.

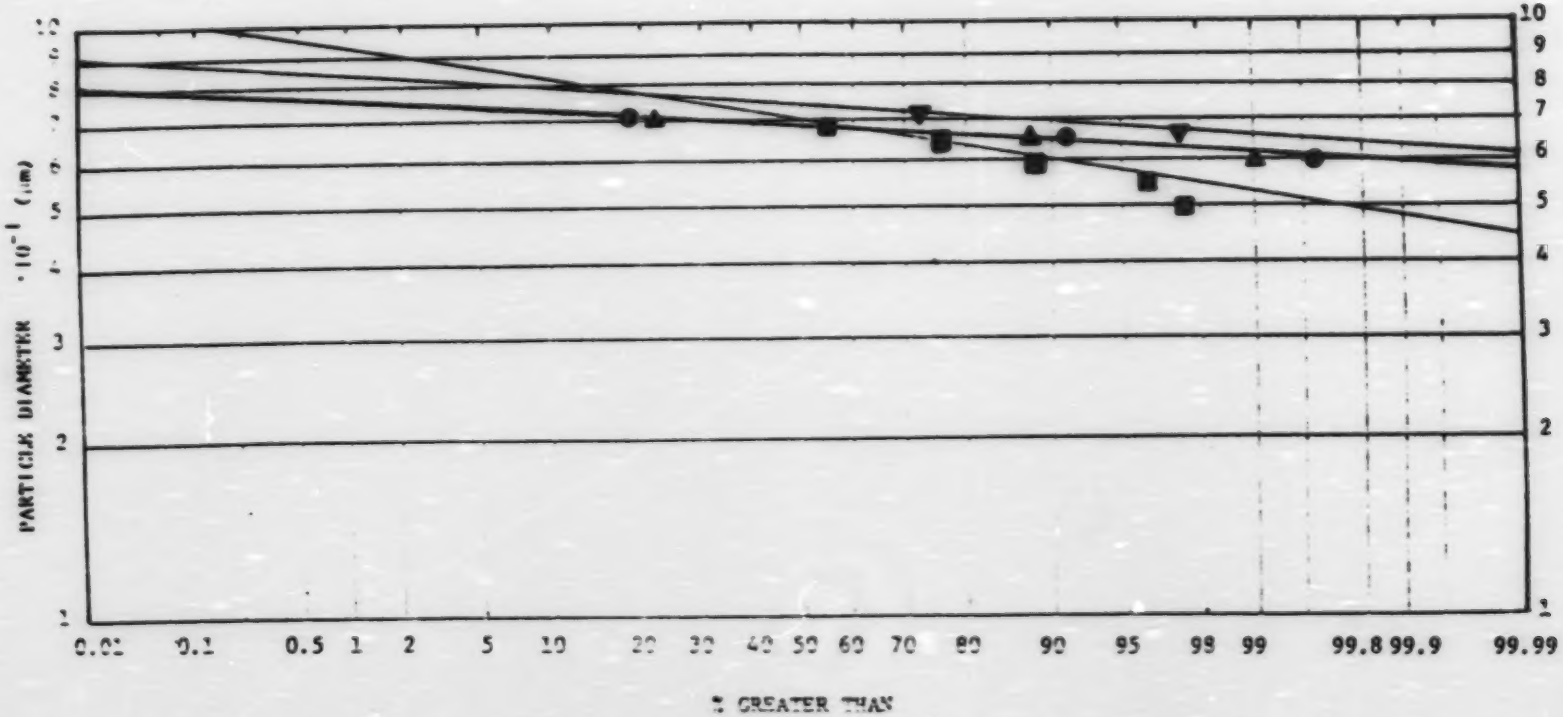

Figure 25. November 25, Flight 1. Track 11, 152 meters AGL altitude. Particle size distribution for histogram 1 (●), 2 (▲), 3 (▼), and 4 (■).

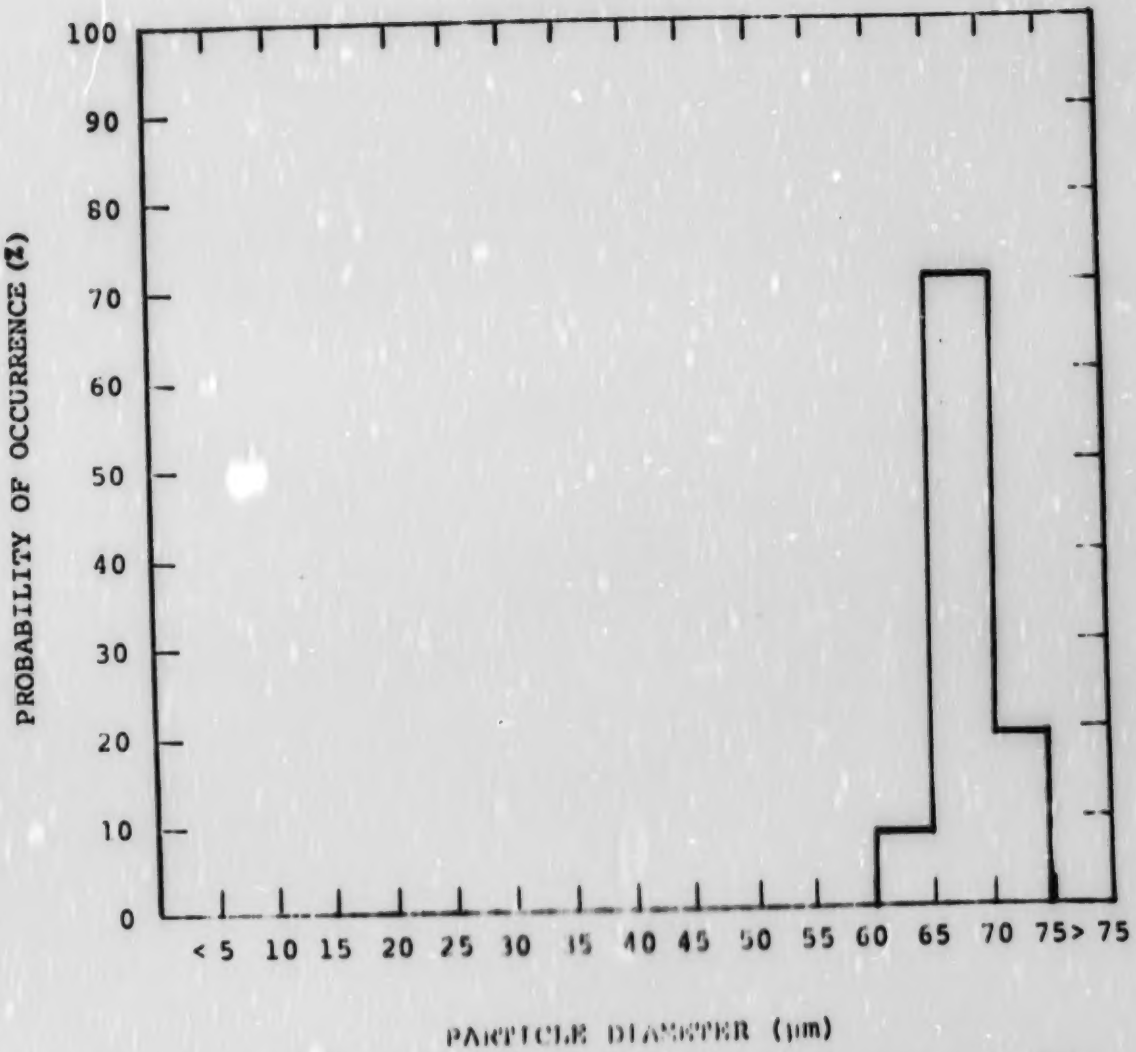

Figure 26. November 25. Histogram 1, Flight 1. Particle Size Distribution.

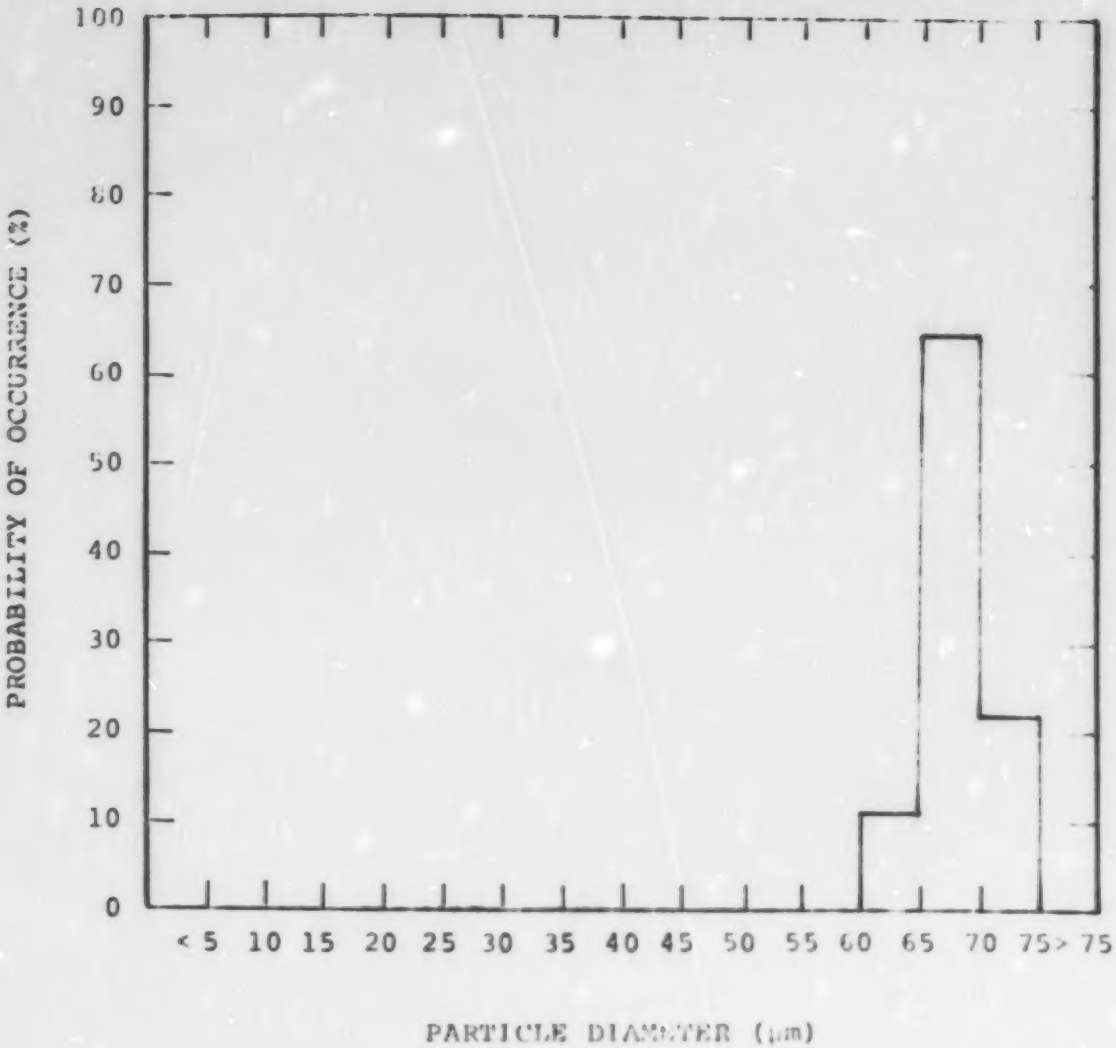

Figure 27. November 25. Histogram 2, Flight 1. Particle Size Distribution.

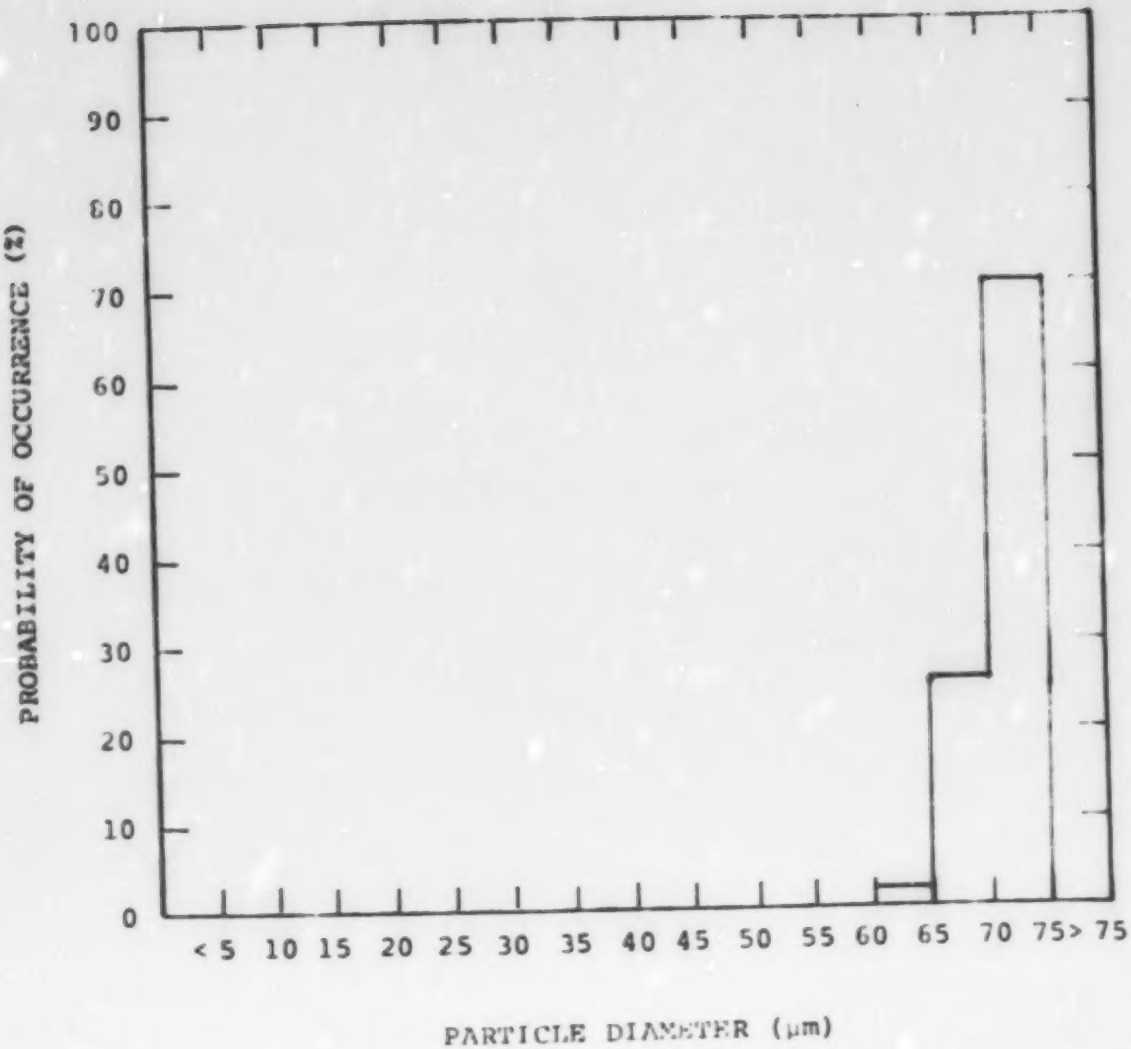

Figure 28. November 25. Histogram 3, Flight 1. Particle Size Distribution.

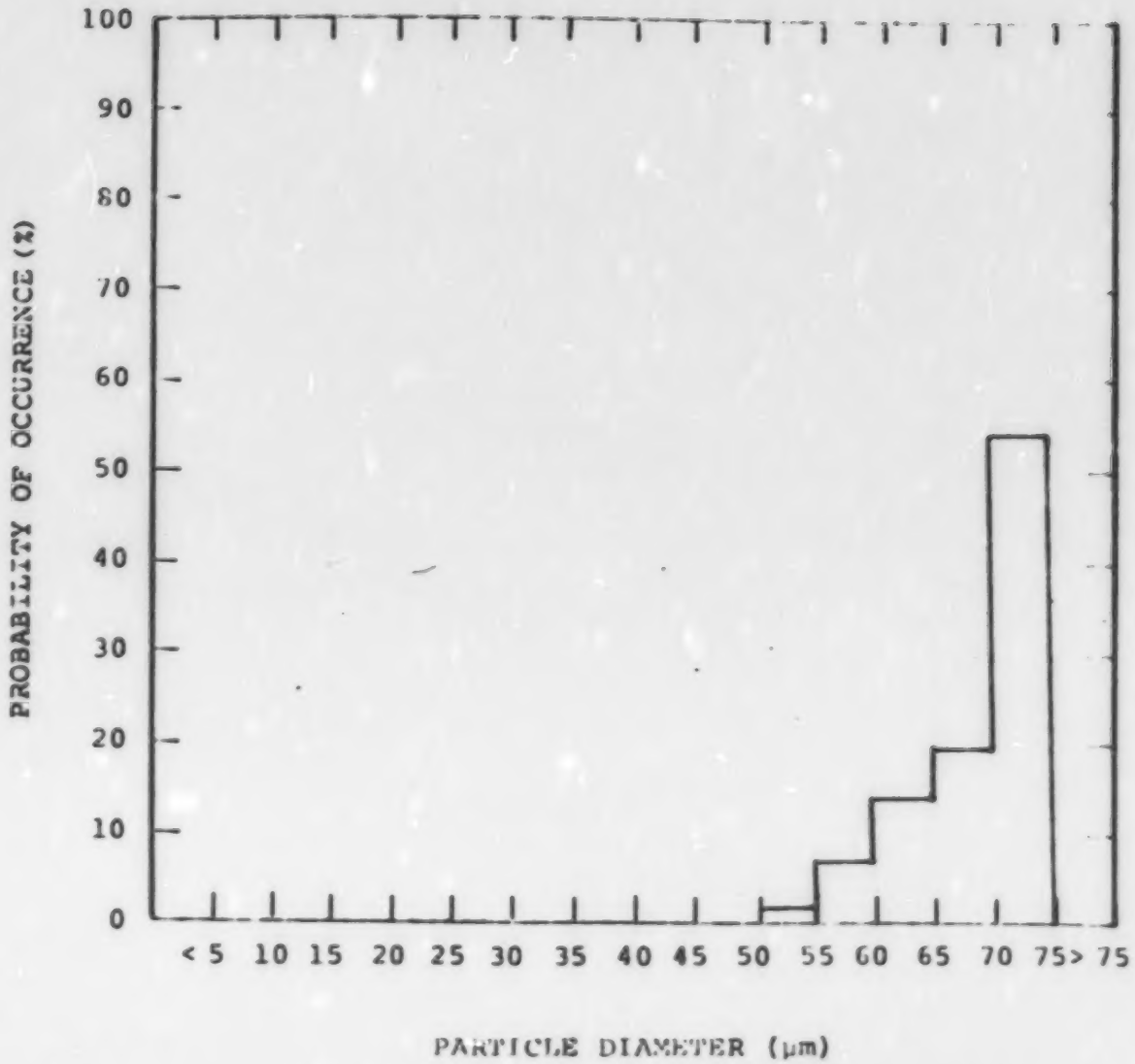

Figure 29. November 25. Histogram 4, Flight 1. Particle Size Distribution.

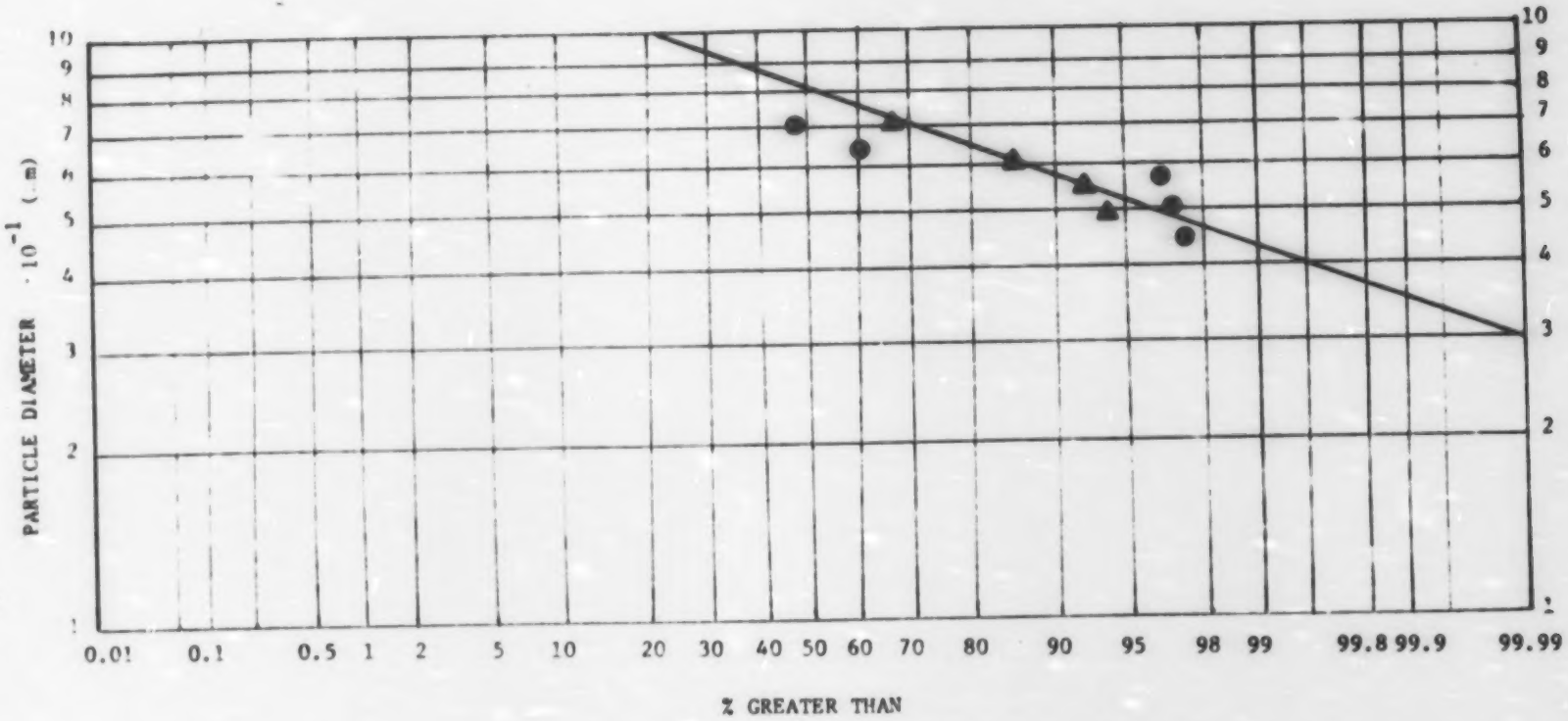

Figure 30. November 25, Flight 1. Last track East of Phoenix. 30.5 m AGL altitude. Particle size distribution for histograms 8 (●) and 9 (▲).

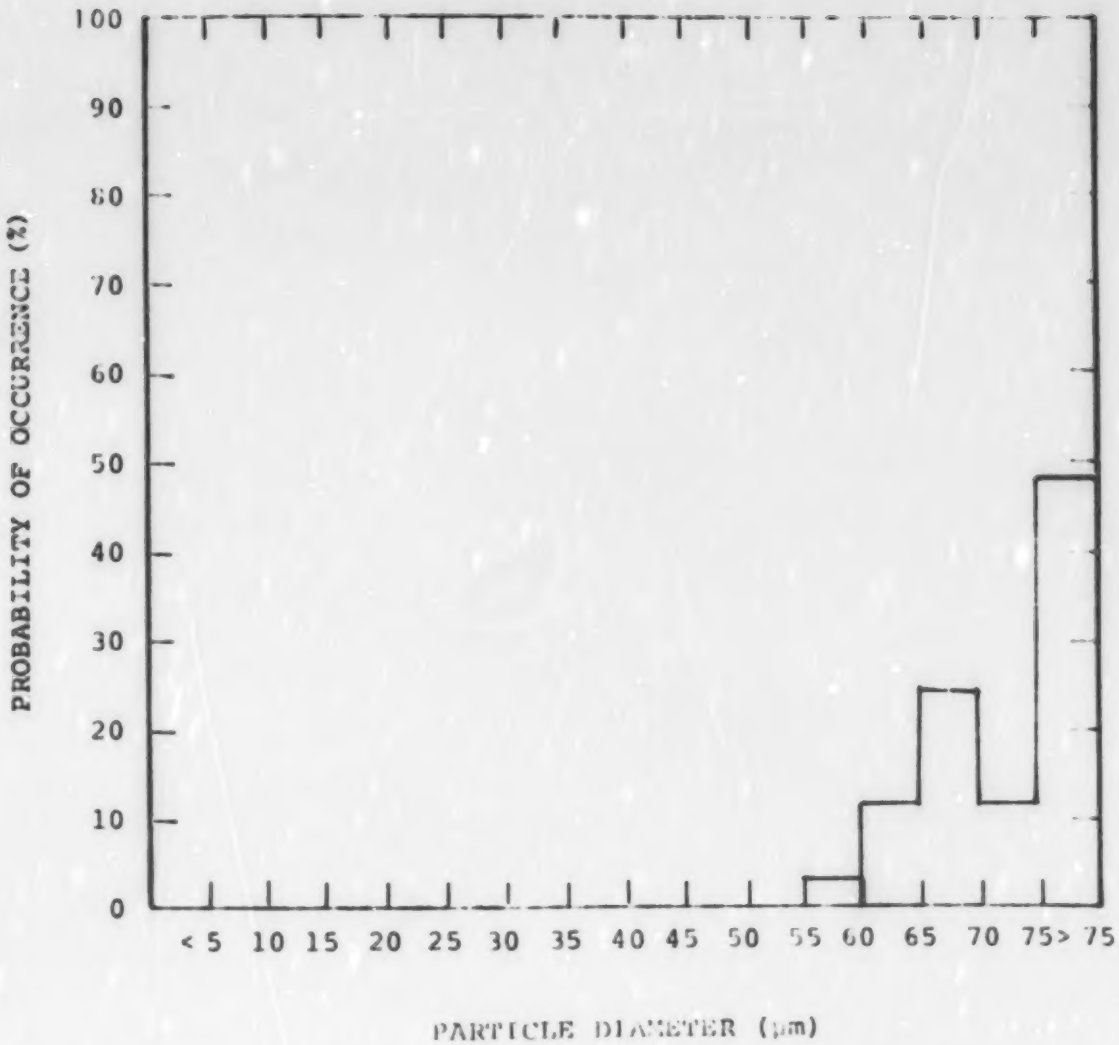

Figure 31. November 25. Histogram 8, Flight 1. Particle Size Distribution.

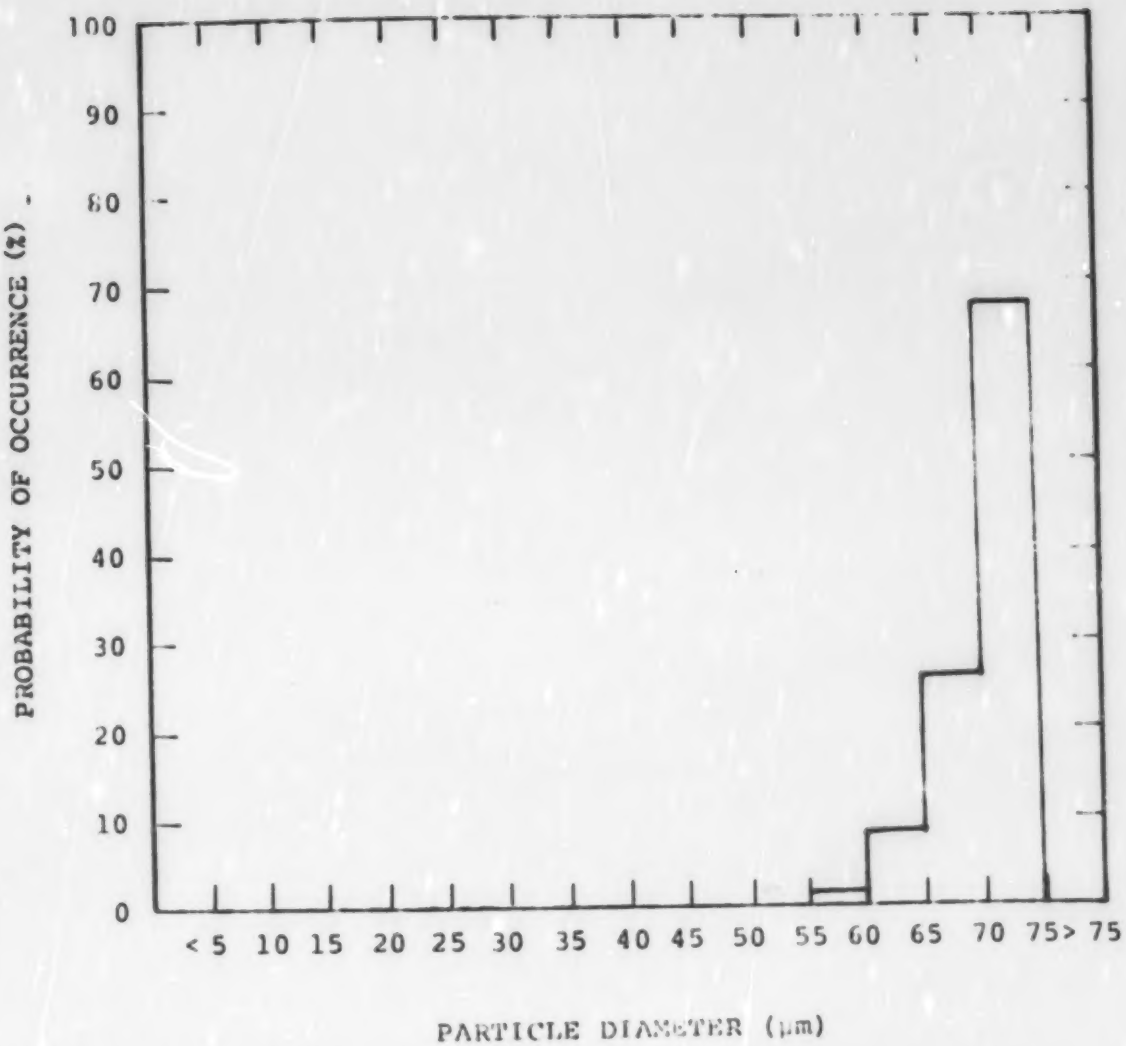

Figure 32. November 25. Histogram 9, Flight 1. Particle Size Distribution.

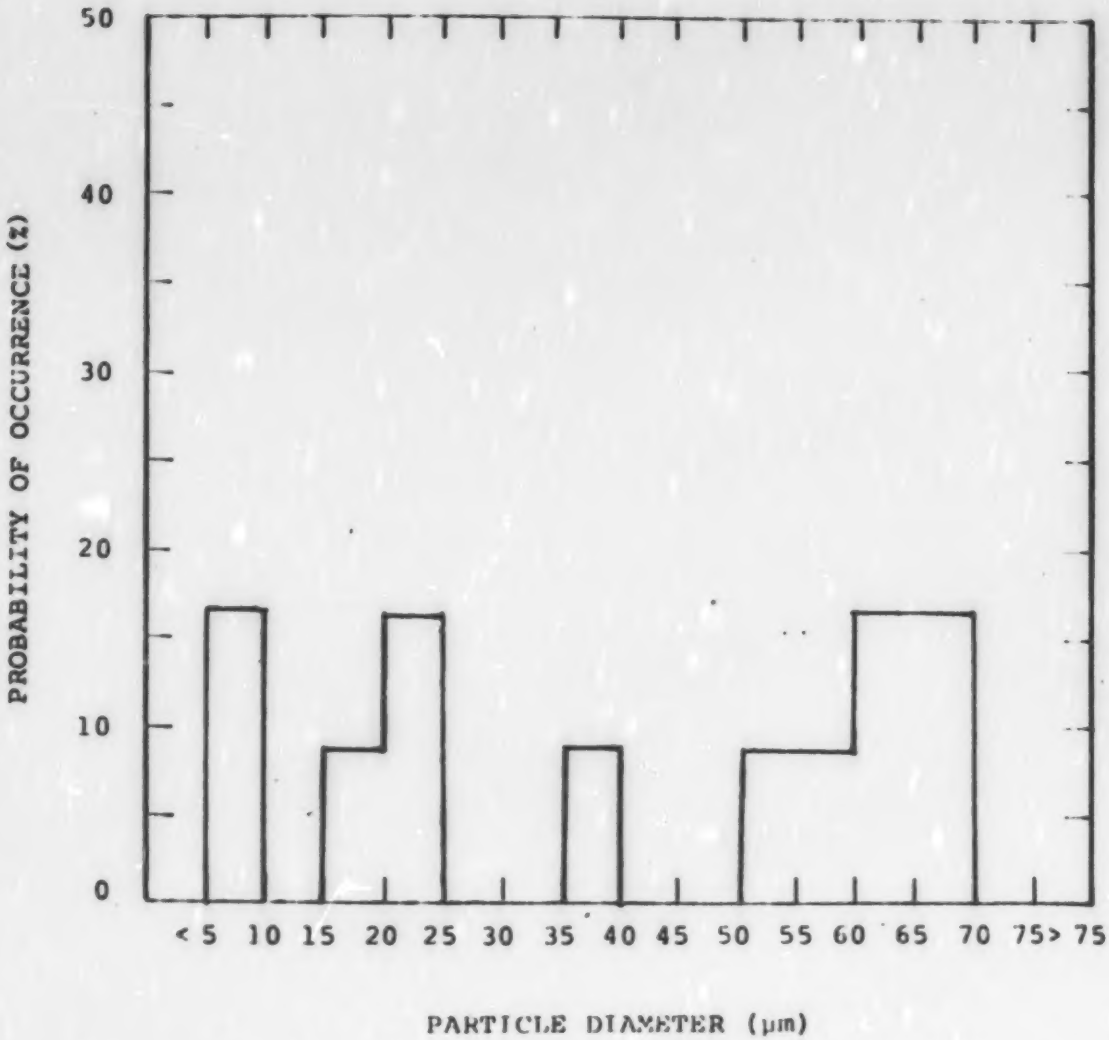

Figure 33. November 25. Histogram 7, Flight 1. Reduced Particle Size Distribution.

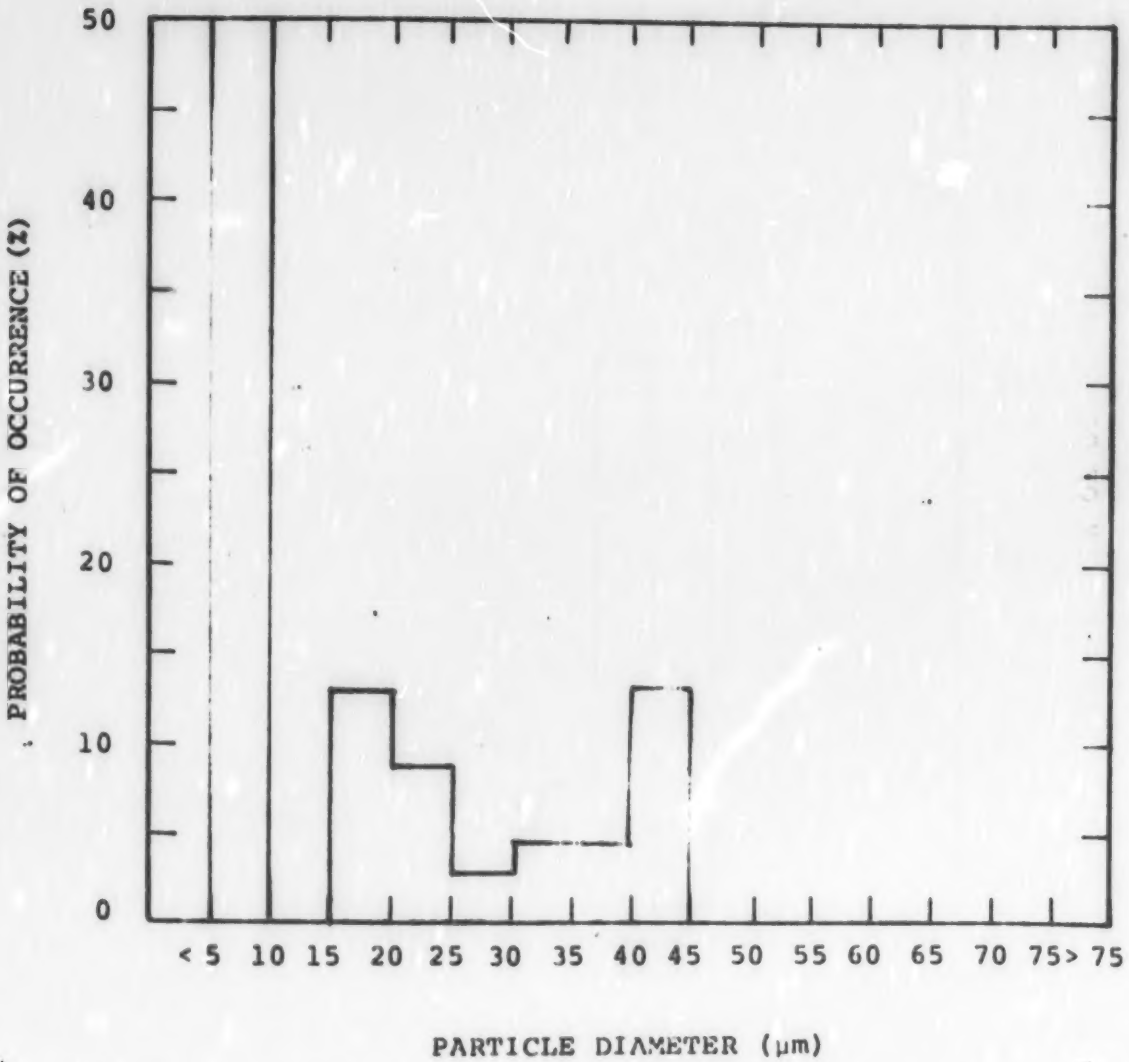

Figure 34. November 25. Histogram 8, Flight 1. Reduced Particle Size Distribution.

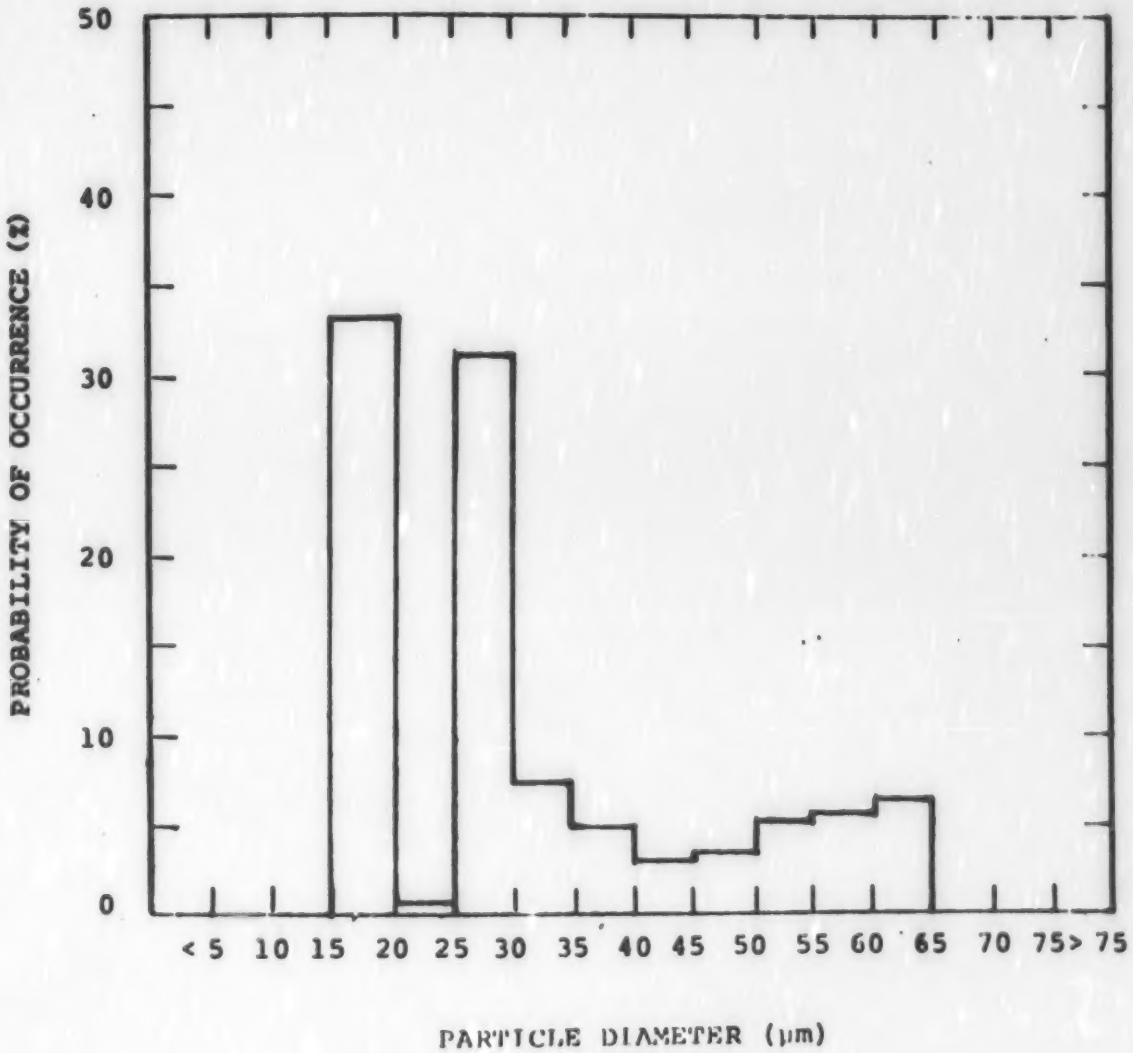

Figure 35. November 25. Histogram 9, Flight 1. Reduced Particle Size Distribution.

Table 10. NOVEMBER 25, FLIGHT 2. PM SYSTEM DATA SUMMARY

Histogram Number	Track	Altitude (Meters AGL)	Flight Notes
1	11	30.5	Threshold: 9.2
2	11	30.5	Repeat of Histogram 1 @ 8.0 Threshold. 519 Second Requisition Time.
3	11	30.5	
4	11	30.5	Velocity Histogram
5	11	229	Possible Sun Noise. Passing Through Brown Cloud. 1720 Sec. Data Acquisition Time.
6	11	457	Heading South Above Brown Cloud.
7	2?	152	Glendale Run. N. Bound 803 Sec. Autosequence.
8			Descent Into Airport @ 152 m/min.

are presented in Figures 36 - 38. The mean size is approximately that observed during the first flight while the standard deviations appear to be slightly broader, although surprisingly narrow compared to what might be expected. Histogram 3 showed results identical to that of Histogram 2. Histogram 4 was a velocity measurement and its results have already been indicated. Histograms 5 and 6 were obtained in the vicinity of an operator-observed "brown cloud". The data from these histograms is shown in Figures 39 and 40 and show a remarkedly narrow distribution with the mode centered between 70 and 75 μm. Histogram 7 represents a series of histograms obtained in continuous 30 sec. intervals over nearly 10 km of horizontal flight path. The modal value observed on nearly all of the histogram sequences was between 70 - 75 μm. Figure 41 shows the relative number density observed along the flight path. The figure clearly shows the high variability of the particle concentration. Two dashed lines are shown on Figure 41. These represent the mean number density observed: (1) with the first 900 m of flight path excluded from the computation and (2) for the entire flight path. The first 900 m of flight path were through an exceptionally dense particle concentration which increased the entire path average concentration. If the first 900 m of path is excluded, the mean number density falls to half that observed for the entire path. These data clearly demonstrate the care that must be exercised in estimating atmospheric particle concentration when averaging over long time intervals or long flight paths.

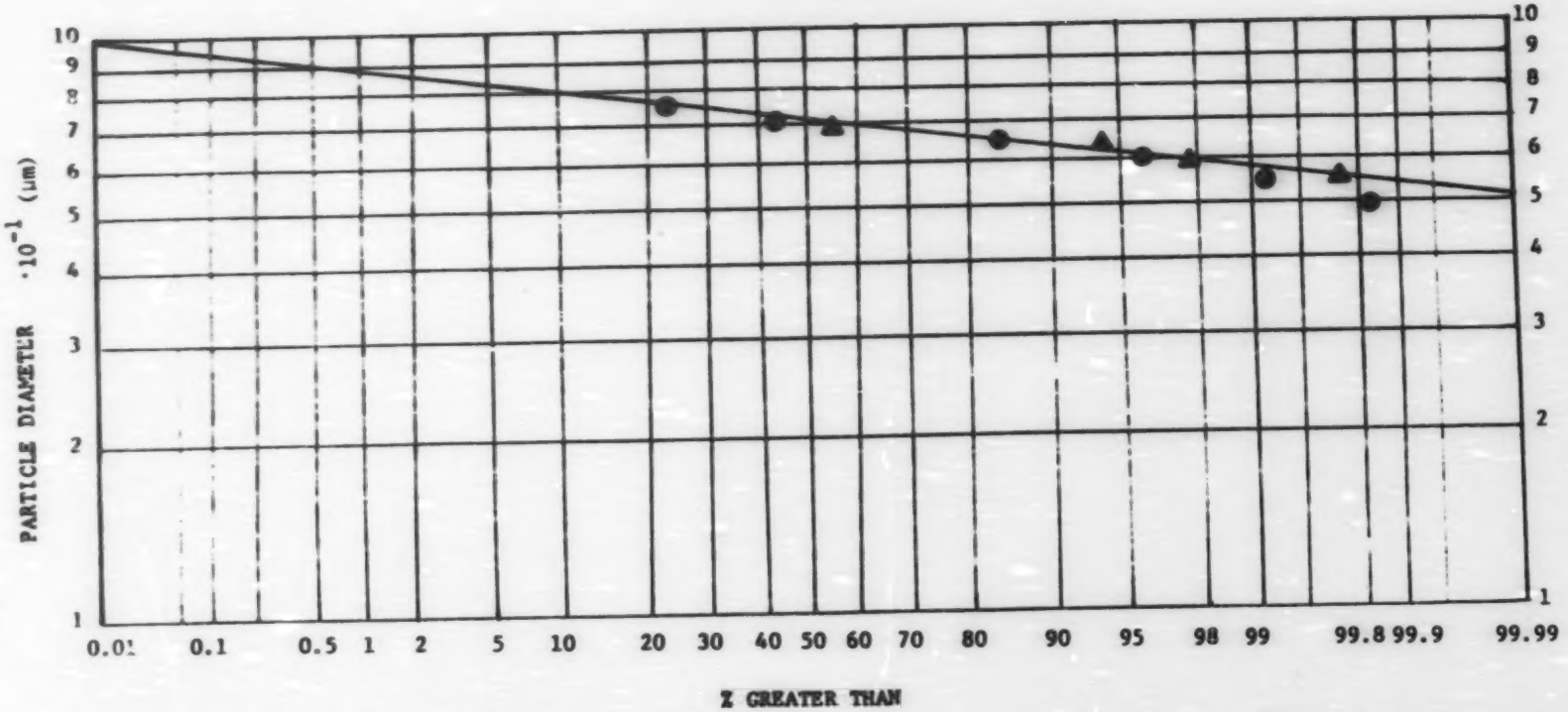

Figure 36. November 25, Flight 2. Particle size distributions for histograms 1 (●) and 2 (▲).

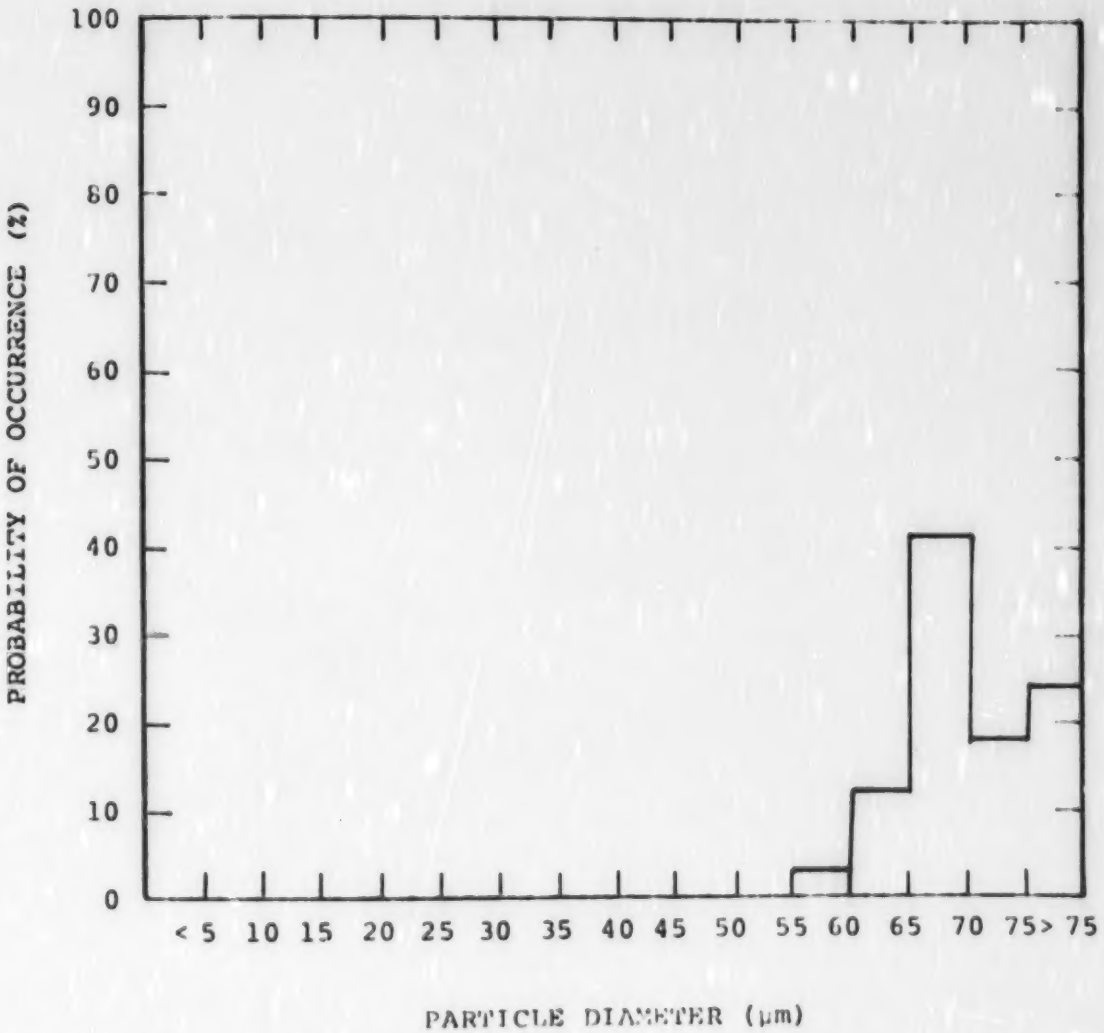

Figure 37. November 25. Histogram 1, Flight 2. Particle Size Distribution.

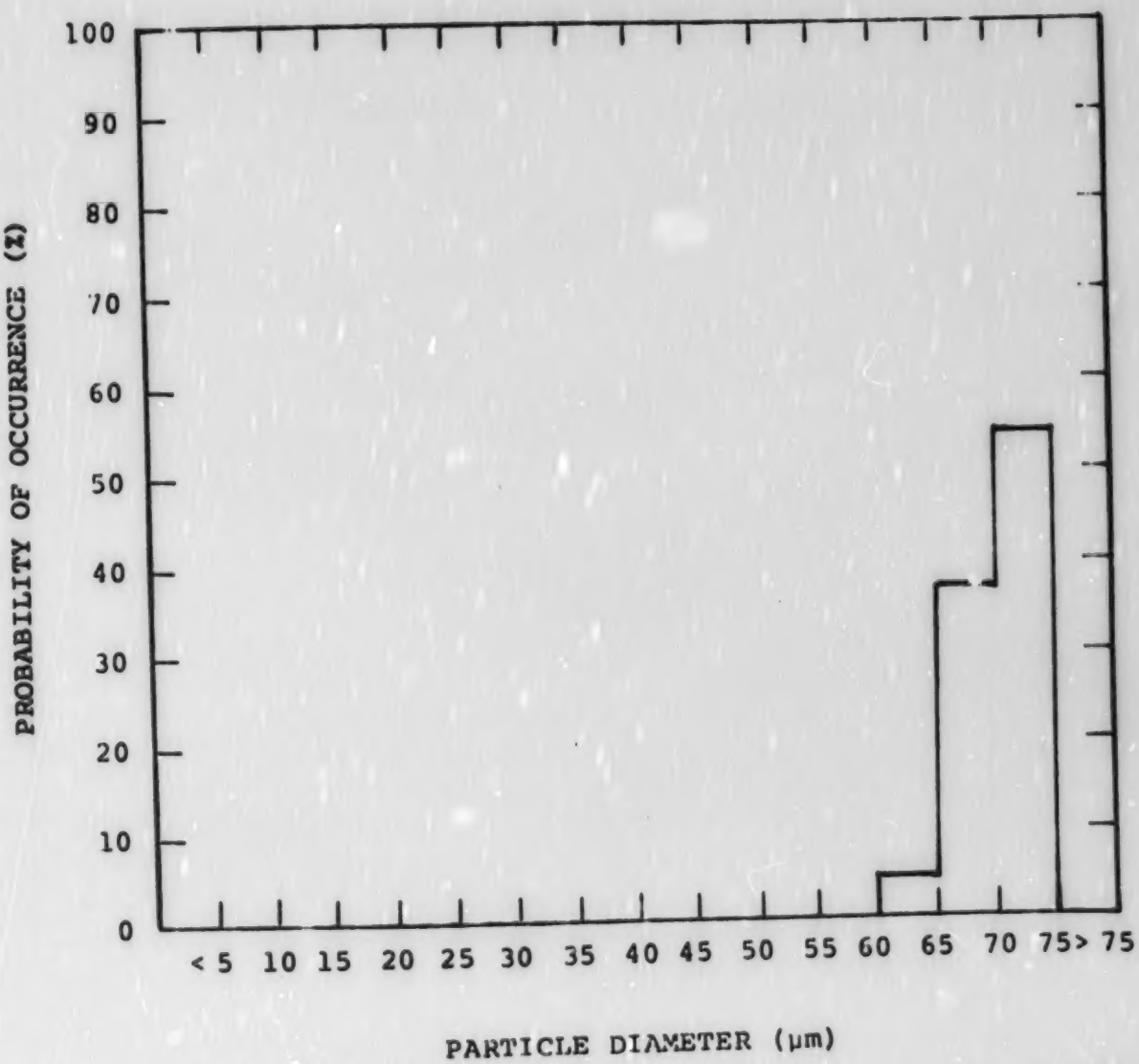

Figure 38. November 25. Histogram 2, Flight 2. Particle Size Distribution.

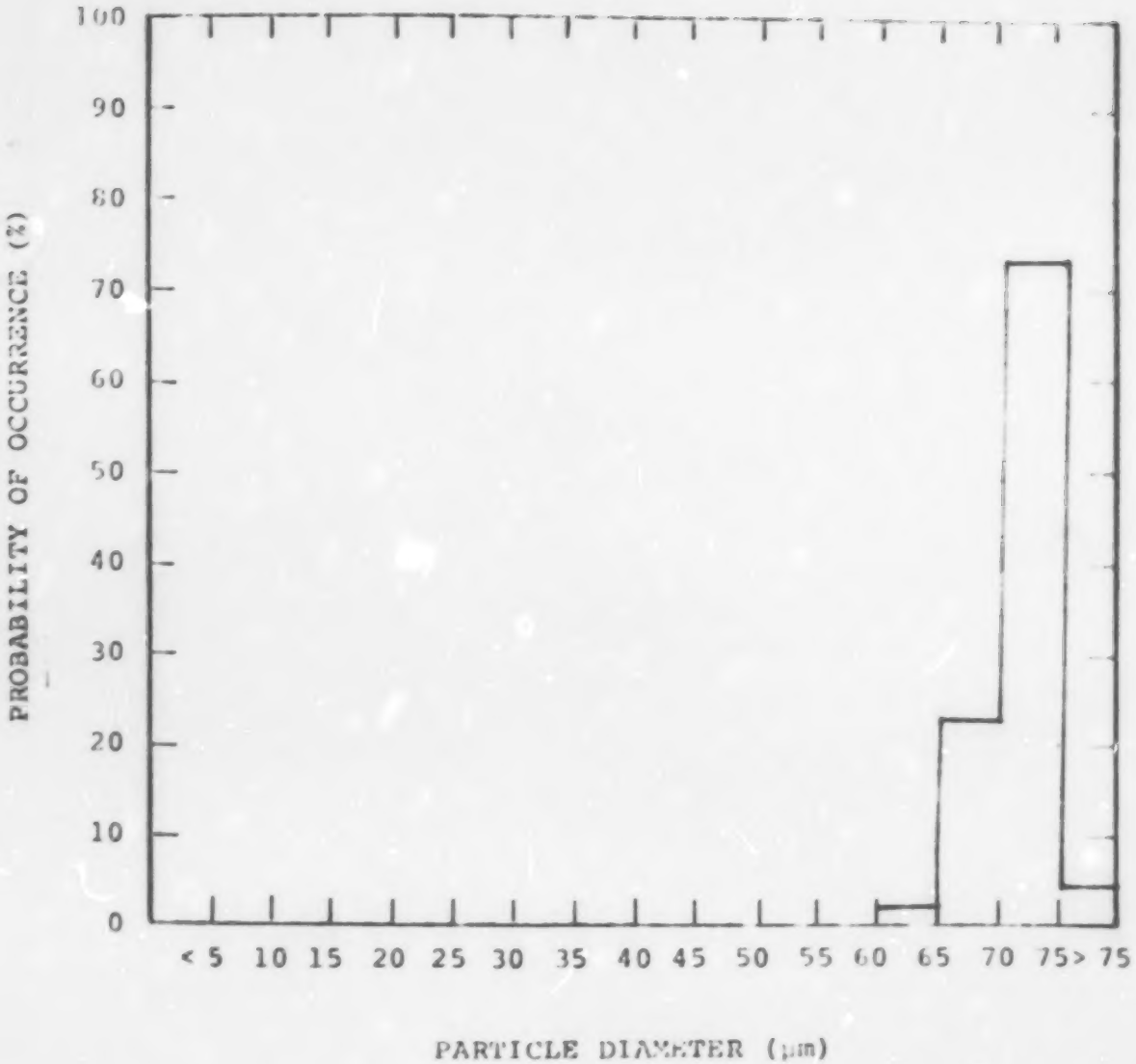

Figure 39. November 25. Histogram 5, Flight 2. Particle Size Distribution.

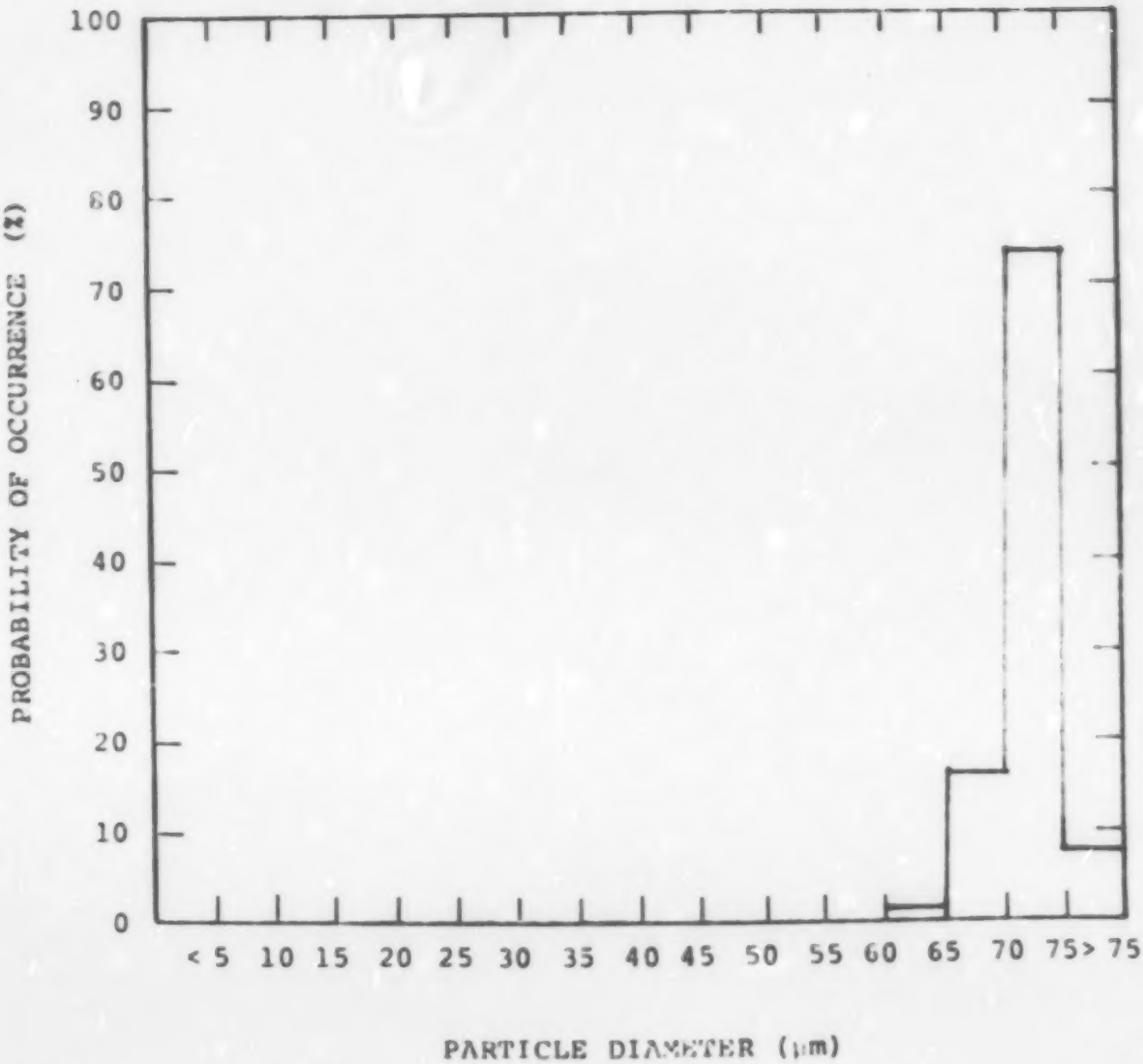

Figure 40. November 25. Histogram 6, Flight 2. Particle Size Distribution.

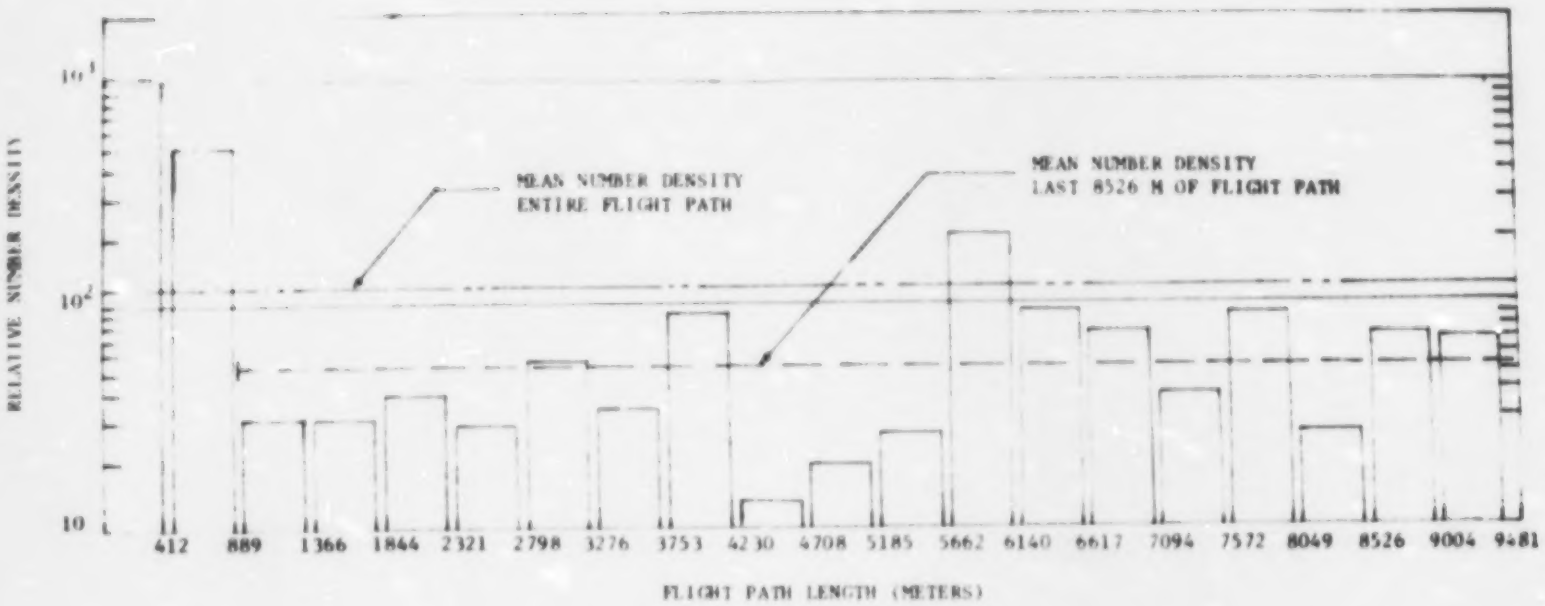

Figure 41. November 25, Flight 2. Track 11 (Glendale), Altitude Is 152 m AGL. Relative Number Density Distribution Over 412 m Distance Increments For A Horizontal Sample Path.

SECTION VIII

CALIBRATION AND ERROR ANALYSIS

The following discussion describes the calibration followed to characterize the response characteristics of the instrument. Potential error sources during its operation in the flight tests and their effects on the resulting measurements are indicated.

CALIBRATION PROCEDURES

It has been well established that for particles where the shape is known that a measurement of the signal visibility gives an accurate measure of the particle diameter. Since a visibility measurement does not depend on the absolute value of the scattered light intensity, there is no need to calibrate the light detector response or the laser power output of the optical system. The primary optical uncertainty in the particle size measurement results from the accuracy with which the fringe period is determined. For beam angles less than 5^{o}, the fringe period may be obtained by using the approximation:

$$\delta = \lambda/\alpha \tag{14}$$

Since the laser wavelength is known to a high degree of accuracy, the only parameter to be measured is the angle between the transmitted beams, α . The measurement uncertainty in this angle is less than 2%. This uncertainty results in the accuracy with which the beam separation can be determined at the transmitting lens. Experience using this measurement technique and then comparing the measurement against that obtained with a direct microscope measurement has shown that such 2% errors are commonly to be expected for fringe periods of the order used in this work.

The electronic system was calibrated by determining how accurately the system could measure a signal of known visibility. The signal calibration input was an electronically synthesized signal which could synthesize the Gaussian shape of real signals to within 5% for the entire duration of the signal. For the signal frequencies encountered during flight operation, it was found that the uncertainty in the visibility was approximately ±1% across the full range of the measurement system. Reference to Figure 4 will show that a ±1% uncertainty in the signal visibility will

correspond to a ±1% relative uncertainty in particle diameter when the particle size is near a fringe period in size. The size uncertainty increases to greater than ±20% when the particle diameter is near 0.1 fringe periods in diameter. Thus, when the particle is comparable to a fringe period in size, the predominate error results from fringe period uncertainty. For sizes near 0.1 fringe periods, the predominate error results from uncertainty in the visibility measurement.

Two flow calibration tests were made with the system. The first calibration test was made with the instrument focused near the center of the inlet to the small wind tunnel at Spectron's Tullahoma facility. The rectangular test section of the tunnel is 10 x 15 cm and is capable of speeds up to 55 m/sec. The airflow was seeded with a water fog and chalk dust combination to simulate flight conditions on the aircraft and to provide a wide variation in signal amplitudes. The PM system clearly demonstrated its ability to respond to the seeded airflow across the entire spectrum of particle sizes. The observed mode sizes were between 25 - 30 μm. The mean velocity was 28 m/sec.

The second flow test occurred during the week following the conclusion of the Phoenix flight test program. In this test, the PM system was used to measure the small particle size distribution of a cloud simulation wind tunnel at UCLA. The tunnel is designed to produce a 2-3 m/sec. laminar airflow under highly controlled temperature conditions. The airflow seeded with a fog having an estimated size distribution ranging between 2 - 30 μm is used to support a 100 μm water droplet. Droplet growth is observed as the small particle distribution droplets collide with the larger drop. In order to cover the required particle size range, the fringe period was changed to 38.7 μm. Impact measurements from gelatin covered glass rods of the small particle distribution were periodically compared with those of the PM system. Typically measured mean sizes were 10 - 12 μm. Excellent agreement was obtained between the two sets of measurements. It was observed, however, that too high a threshold setting could bias the distribution toward the larger sizes. A suitable threshold setting was found to be less than 6.8, this is not unrealistic in view of the particle size range being examined.

ERROR ANALYSIS

The errors associated with these measurements may be divided into two categories - those inherent in the PM measurement technique, and those which arise from the way in which the PM system is applied. The following discussion is centered around these two classifications.

INHERENT MEASUREMENT ERRORS

A visibility measurement can only be directly associated with a measure of particle size when the shape of the particle is known. All data evaluation presented in this paper has assumed a spherical particle shape. Clearly, atmospheric dust particles are not spheres. Hence, the measured visibilities represent some average particle dimension for particles with presumably random shapes. Even if the particles have reasonably well defined shapes (e.g. cylinders), it is to be expected that they will be observed in all orientations so that an averaging estimate must be used for all possible particle orientations. Such averages have not been computed. Thus, valid estimates between the assumed diameter using a spherical particle visibility function versus size estimates for a randomly shaped or randomly oriented particle visibility function cannot be made. It is clear, however, that the visibility function for a sphere should represent the asymptotic limit for a large number of measurements of a randomly shaped particle observed for a continuum of orientation angles.

The equivalent diameter of the estimate should be expected to approximate the maximum diameter of the particle. Thus, the spherical particle visibility function is assumed to be a good approximation when a large number of measurements occur in any one size increment in the histogram distribution.

The calibration procedures discussed in Section VIII ensure that the PM system accurately measures a particle even when the signal-to-noise ratio is low. The PM system electronics are designed with logic circuits which cause the instrument to reject erroneous or overly noisy signals. When the signals become too noisy, the data rejection rate becomes high with subsequently few measurements obtained by the instrument. A primary source of noise is the shot noise generated by background light incident on the photomultiplier tube. The background light may result from stray laser light not associated with the signal or from broadband environmental sources such as the sun. Laboratory tests of the PM system showed that

the only stray laser light sources are those which result from light scattered out of the beams transmitted to the sample space. This light is only observable when the particle number density becomes several hundred per cc. For the Phoenix flights, this condition did not exist. Sunlight, however, did present a problem. A 10 nanometer interference filter was originally used in the instrument and was found to be adequate in laboratory simulations with bright lights. For example, a standard 3 cell flashlight could be pointed almost directly into the PM receiver with no noticeable effect. A measure of the flashlight power output indicated that it should produce a mean power output comparable to that of commonly accepted sunlight figures. However, it was found that between the hours of about 9 AM and 3 PM on clear sunny days in Phoenix, the 10 nanometer filter required instrument operation at very high threshold levels. Such levels were found to bias the system towards large particle measurements in the UCLA flow tests. Comparison of night flight data where the threshold was set to a low value (4.5) to those of day flights did not reveal significant changes in the distribution functions. From this field application it is estimated that a filter with a 1 nanometer bandpass should be more than adequate for nearly all sun conditions that would be encountered with an instrument of this type. This type of filter is a commonly produced item but could not be acquired in time for use in the test program. A second 10 nanometer filter was obtained, however, and used with the filter originally in the system. It is estimated that the passband of the two filters was about 70 nanometers. This filter combination proved to be sufficient for a relatively low threshold during the high sun hours.

Errors were also found to result due to radiative pickup during radio transmission while the PM was in flight. However, the system was equipped with an amplifier to preserve signal shape fidelity between the electronics system and the photomultiplier tube. By adjusting the capacitance in the amplifier this source of error was eliminated.

In order for accurate measurements to be obtained, it is necessary that the optical system maintain paraxial alignment. Since the optical system was attached to the instrument rack which is shock mounted, no alignment difficulties were experienced during the entire test program.

APPLICATION MEASUREMENT ERRORS

It is difficult to evaluate application measurement errors. They resulted, in this application, from the data bias introduced by the flow field pattern around the aircraft. It is clear from the velocity measurements

obtained while the PM system was in flight that the sample space of the instrument either was well within the boundary layer of the aircraft or was shadowed by the wheel strut. The particle size distributions obtained with the PM system show indications of being artificially separated or sieved before they were measured. Small values of the distributions' standard deviations and the relatively large values of the mean particle size seem to make the data suspect. Furthermore, PM measurements obtained on the ground prior to takeoff seem to indicate about the same mean particle size as the airborne measurements but the ground based measurements reflect higher concentration of smaller particles than the airborne measurements. This effect is opposite to that generally thought to exist, i.e. the airborne measurements should show an increased number of small particles, since the larger particles would be expected to fall out while the smaller ones would remain aloft. This was generally observed to be the case on the test flight flown November 19 and in histograms obtained on November 22. However, on subsequent flights, it was found that the particles were distributed uniformly in size except for the very shallow inversion layers which were observed. While it is possible that a high threshold setting to avoid background light noise biased the distribution towards the larger particle sizes, the possible sieving effects of the aircraft flow field should not be discounted. U. S. Air Force studies have shown that an aircraft boundary layer tends to cause particle size separation to distances as large as 2 - 3 fuselage diameters. These studies were for particles greater than 50 μm in diameter and for aircraft flying at speeds of about 120 knots at relatively high altitudes. While the aircraft in this case flew at significantly slower speeds and altitudes, the data obtained by the PM system strongly suggests that a careful evaluation of such effects is in order.

An alternative explanation of the data differences in the inflight and ground level measurements is suggested by assuming that a general suspension of larger particles exists over the county from farms and dirt roads. The particle distribution at near ground level altitudes is then probably governed by auto traffic on paved roads. The grinding action of tires reduces the mean value of the general suspension and broadens the distribution.

REFERENCES

1. Y. Yeh and H. Z. Cummins, Appl. Phys. Letters 4, 126 (1964).

2. D. B. Brayton and W. H. Goethert, Trans. Inst. Soc. Am., 10, 41 (1971).

3. R. S. Goldstein and D. K. Kried, J. Appl. Mech., (E) 4, 813 (1967).

4. F. Durst and J. H. Whitelaw, Proc. Roy. Soc. Londa A., 324, 157 (1971).

5. W. M. Farmer and J. O. Hornkohl, Appl. Optics 12, 2636 (1973).

6. W. M. Farmer, "The Interferometric Observation of Dynamic Particle Size, Velocity and Number Density" Ph.D. Thesis, (College of Liberal Arts, The University of Tennessee, 1973).

7. F. Durst, "Development and Application of Optical Anemometers," Ph.D. Thesis (Heat Transfer Section, Dept. of Mech. Engr., Imperial College London, S.W.1., 1972).

8. R. M. Fristrom, et.al., Faraday Symposia Of The Chemical Soc., No. 7, 183 (1973).

9. W. M. Farmer and D. B. Brayton, Appl. Opt., 10, 2319 (1971).

10. F. L. Crosswy and J. O. Hornkohl, Rev. Sci. Instrum., 44, 1324, (1973).

11. W. M. Farmer, Appl. Opt. 13, 610 (1974).

12. J. D. Trolinger, "Laser Instrumentation For Flow Field Diagnostics" AGARDograph No. 186. (1974).

Preceding page blank

APPENDIX. Daily Log

The following is a daily log kept by Spectron personnel of the day to day operation during the EPA particle morphokinetometer test program.

NOVEMBER 17

The system equipment arrived in Phoenix and was picked up at 1500 hours. Jeff van Ee indicated in a prior discussion that he would not want to have the equipment placed on the helicopter that day since a mission was being flown during the afternoon. The equipment was uncrated and set up at the motel and appeared to work properly and to generate signals from dust in the air.

NOVEMBER 18

The equipment was taken to the helicopter at 0800 hours. An attempt was made to fit the optical system to the helicopter with the bracket built for it by the EPA/Las Vegas. The bracket material was found to be too flimsy to support the optical system. The helicopter was scheduled to fly a mission beginning at 1100 hours and returning at 1300 hours. During this time, 2.5cm x 2.5cm x 0.31cm aluminum angle was purchased at a hardware store and a more substantial bracket was built by Spectron using the EPA bracket as a pattern. At 1330 hours, the optical system was mounted on the helicopter using the new bracket. It was found to be sufficient. The electronics system (except for the oscilloscope) was strapped in place on the instrument rack and connected. Jeff van Ee was instructed an hour to program the histogram generator of the PMAC 554 and the system was given an initial shakedown flight to discover any mechanical or electronic defects. This flight lasted from 1515 hours until 1800 hours. Upon return, all systems appeared to be functioning normally. Some data printout was obtained. However, it was not considered reliable since no oscilloscope observations were obtained to determine the threshold necessary to limit noise from background light.

Preceding page blank

NOVEMBER 19

The optical system was reinstalled on the aircraft and optical alignment checked. The oscilloscope was rack-mounted at this time. A system check indicated a high level of noise due to background light. A 10 nanometer interference filter was installed on the front of the PMT slit aperture. The filter appeared to be sufficient for high threshold operation of the PMAC 554. The digital recorder began to print in a sporadic manner. The Costa Mesa office was contacted in an attempt to locate a replacement recorder after all attempts to find one in Phoenix failed. In order to verify that all the other systems functioned properly, Hornkohl and Farmer took a test flight with the pilot, Don Nail, around the edge of Phoenix in the Chandler area. The PMAC 554 appeared to work well. Hornkohl set a maximum threshold level and was still able to obtain very high quality signals. Direct sunlight shining towards the optical system provided too great a background for operation. However, with the helicopter oriented such that at least a 45 degree zenith angle relative to the optical axis was maintained, the system functioned acceptably well. During this flight, typical data rates were 10 to 200 acquired measurements per second. Passes were made across an agricultural area next to the desert. There appeared to be a considerable amount of dust above some of the agricultural fields which were flown over. Visual observation of the digital displays indicated expected data trends (e.g. smaller particle sizes were observed at a 152 m. altitude than at a 30.5 m. altitude). In the area next to the desert, three passes were made - one at 152 m., one at 91.5 m., and one at 30.5 m. Data was also generated on the return leg of the test flight. The altitude at this time was 152 m. and flight speed was 42 m/sec (80 knots). Even though the printer output was sporadic some usable data was obtained.

NOVEMBER 20

A Hewlett Packard Model 1055A recorder was received from the Costa Mesa office. It was tested with the electronics and found to function properly.

NOVEMBER 21

The optical system was reinstalled on the helicopter at 0615 hours. Temperature was 7.2°C. The optical system had been left in the trunk of the rental car all night and was too cold to start (laser would not lase).

Also it was found that the digital recorder printed incorrect digits from the histogram generator. The laser power supply was left on and the system flown as was in the hope that the laser supply would sufficiently warm the optics box to make the laser start. Upon return from the early morning flight, both the laser and the printer functioned. A second test flight was flown during the afternoon beginning at 1500 hours with Hornkohl and Farmer on board the helicopter. Immediately after the system became airborne, Hornkohl could not observe signals on the oscilloscope. The helicopter was returned to the airport and system alignment checked. It was found to be satisfactory. Hornkohl changed the capacitance in the PMT tube signal output amplifier to eliminate occasional circuit oscillations induced by radio transmission. Flight resumed at 1540 hours. Some initial passes were made over fields in the Chandler area which were being cultivated. The observed data rate was very low. Approximately 1/3 of the flight path 11 was flown in a 10 second autosequence mode. The data rate was so low that the autosequence mode was changed to a 30 second sample time. Additional passes were made over other agricultural fields in this autosequence mode. The observed data rate was at least a factor of 10 less than that observed on the 19th. However, the atmospheric visibility was considerably higher this date than on the 19th. Flight returned to the airport at 1630 hours. The optical system was returned to the motel and the transmission alignment was checked since it could possibly have been changed in attempting to start the laser in the early morning hours. Paraxial alignment was found to be about 5 degrees off. It is also possible that the position of the light filter was such that the bandpass of the filter greatly attenuated the amplitude from the small particles. However, rotational tests of the filter in the laser beam indicated that this was probably not the case.

NOVEMBER 22

The optical system was installed on the aircraft at 1100 hours. By AC coupling the oscilloscope, it was determined that the system was responding to airborne particles but that background light induced by the high sun angle was inducing an exceptionally high noise level. The only signals that could be observed were those from exceptionally large particles. An attempt was made to reduce the background light by using additional red celluloid with the 10 nanometer interference filter. The mission lasted from 1200 hours to 1500 hours. The data recorded in almost all cases fell in the greater than 20 - 25 μm histogram bin.

One histogram obtained at a 305 m. altitude appeared to have a broad distribution. A second flight was begun at 1600 hours and returned at 1800 hours. During operation with a low sun angle, Jeff van Ee was able to adjust the system to a much lower threshold and a high data rate was obtained. The measurements, however, consistently fell in the particle size bins greater than 65 μm.

NOVEMBER 23

Instruments in the aircraft were turned on at 1600 hours for an early morning mission on November 24. The optical system was installed at 2100 hours and left on. The atmosphere was exceptionally clear (local radio reports indicated that atmospheric visibility was 113 Km). There appeared to be a shallow inversion layer close to the ground. The signal threshold level was set to 8 for the initial flight. Flight return was at approximately 0100 hours, November 24. The system recorded very little data although it seemed to be functioning normally. Histograms taken on the ground both before and after the flight showed a particle size distribution usually observed on a day-to-day basis. The system was left on for the 0400 November 24 mission.

NOVEMBER 24

Flight takeoff was at 0400 hours. Farmer rode as co-pilot to ask van Ee to vary different system parameters in order to discover any possible system malfunctions. During the first data pass, various thresholds were attempted with essentially identical results. A threshold level 4.5 was chosen because such a level was found to be acceptable in all calibration tests and did not appear to induce any data bias. During the flight, the observed data rate was again exceptionally low compared to that of November 19. On the return flight to the airport, the pilot was requested to descend at a rate of 76 m. per minute from an altitude of 366 m. van Ee was requested to set the PMAC 554 at autosequence mode and to sample every 10 seconds. Visual observation of the acquired data rate indicated an inversion layer somewhere between 30.5 and 15 m.

NOVEMBER 25

An additional 10 nanometer interference filter was received from the Costa Mesa office. With both filters used together it was estimated that a passband of 70 nanometers could be received with about 25% transmission. Both of these filters were used in the system. To compensate for the reduced transmission losses, the sample space of the optical system was moved closer to the receiver window (28.6 cm). The sample space appeared to sit immediately behind the wheel strut. Takeoff was at 0700 hours and return was at 0930 hours. The threshold was set to about 9.2. van Ee reported observing good signals on the oscilloscope and numerous counts (typically 10,000) were recorded in the histogram. The second mission takeoff was at 1030 hours. van Ee was requested to obtain a velocity histogram and to record some data in a 10 second autosequence upon descent. Upon return, the aircraft had to abort the straight-in descent and make a circular pass about the airport. Aircraft return was at approximately 1230 hours. The PM system appeared to generate considerable data. There was a slight overcast due to high cirrus clouds which also probably significantly contributed to the reduction of background sunlight. The equipment was packed at 1300 hours and sent to shipping.